Texas A&M Transportation Institute

Verification of ASR Resistance Property of the Selected Concrete Mix Designs by the Precast Industries in Texas: Technical Report

Technical Report 5-6656-01-R1

Cooperative Research Program

TEXAS A&M TRANSPORTATION INSTITUTE
COLLEGE STATION, TEXAS

in cooperation with the
Federal Highway Administration and the
Texas Department of Transportation
http://tti.tamu.edu/documents/5-6656-01-R1.pdf

Technical Report Documentation Page

1. Report No. FHWA/TX-19/5-6656-01-R1	2. Government Accession No.	3. Recipient's Catalog No.
4. Title and Subtitle VERIFICATION OF ASR RESISTANCE PROPERTY OF THE SELECTED CONCRETE MIX DESIGNS BY THE PRECAST INDUSTRIES IN TEXAS: TECHNICAL REPORT		5. Report Date Published: September 2021 6. Performing Organization Code
7. Author(s) Anol Mukhopadhyay, Kai-Wei Liu, Mostafa Jalal, and Jia-Lin Hsu		8. Performing Organization Report No. Report 5-6656-01-R1
9. Performing Organization Name and Address Texas A&M Transportation Institute The Texas A&M University System College Station, Texas 77843-3135		10. Work Unit No. (TRAIS) 11. Contract or Grant No. Project 5-6656-01
12. Sponsoring Agency Name and Address Texas Department of Transportation Research and Technology Implementation Office 125 E. 11th Street Austin, Texas 78701-2483		13. Type of Report and Period Covered Technical Report: September 2018–August 2019 14. Sponsoring Agency Code

15. Supplementary Notes
Project performed in cooperation with the Texas Department of Transportation and the Federal Highway Administration.
Project Title: Verification of ASR Resistance Property of the Selected Concrete Mix Designs by the Precast Industries in Texas
URL: http://tti.tamu.edu/documents/5-6656-01-R1.pdf

16. Abstract

The Texas A&M Transportation Institute conducted the development and validation of alkali-silica reaction (ASR) testing as well as the approach for formulating ASR-resistant concrete mixtures in Texas Department of Transportation (TxDOT) Projects 0-6656 (ASR Testing: A New Approach to Aggregate Classification and Mix Design Verification) and 0-6656-01 (Further Validation of ASR Testing and Approach for Formulating ASR Resistant Mix). Specifically, development and validation of two innovative ASR test methods and a combined performance-based approach with four recommended steps were performed in these two previous projects. In Step 1 of the performance-based approach, determination of the aggregate ASR composite activation parameter (CAP) and threshold alkalinity (THA) using a rapid aggregate chemical test called the volumetric change measuring device (VCMD) is performed. Formulation of an ASR-resistant mix by applying mix design controls depending on CAP-based reactivity prediction, THA, and some consideration of the severity of ambient conditions is conducted in Step 2. In Step 3, mix design adjustment/verification based on the THA–pore solution alkalinity (PSA) relationship (e.g., PSA needs to be below THA to prevent/minimize ASR) is recommended to perform as an optional control. Concrete mix design validation using a newly developed accelerated concrete cylinder test (ACCT) is part of Step 4. The main objective of this study was to verify the ASR resistance property of the selected concrete mix designs of bridge girders by the precast industries in Texas by applying the above-mentioned combined performance-based approach.

It seems that the selected precast mix designs with 20 percent Class F fly ash are sufficient to prevent ASR. Although the ACCT method creates accelerated conditions, dense microstructural development of the precast concrete can affect ASR expansion in the following ways: (a) minimize ASR expansion (especially at the early ages) compared to conventional concrete due to reduced rate of ionic movement (lesser degree of ASR) inside the concrete specimen as well as negligible penetration of soak solutions/ions from the soak solution into the specimen, and (b) enhance ASR due to the relatively higher PSA because of the use of low w/cm. Continuation of ACCT testing for a longer period (more than 75 days) is recommended to ensure a reliable verification. The application of this combined innovative approach to verify and fine tune (if needed) the precast mix designs has the potential to provide favorable life-cycle costs and a tangible measure of how TxDOT is fulfilling its mission to provide a safe and reliable transportation system to the citizens of Texas. However, additional implementation work using this combined approach is recommended to test different job concrete mixes containing different supplementary cementitious materials (e.g., Class C fly ashes, blended ashes, slag, etc.) to validate ASR-resistant concrete mix designs for different applications.

17. Key Words	18. Distribution Statement
Alkali-Silica Reaction (ASR), Precast Mixes, Bridge Girders, ASR-Resistant Concrete Mixture, Concrete Durability	No restrictions. This document is available to the public through NTIS: National Technical Information Service Alexandria, Virginia http://www.ntis.gov

19. Security Classif. (of this report)	20. Security Classif. (of this page)	21. No. of Pages	22. Price
Unclassified	Unclassified	54	

Form DOT F 1700.7 (8-72) Reproduction of completed page authorized

VERIFICATION OF ASR RESISTANCE PROPERTY OF THE SELECTED CONCRETE MIX DESIGNS BY THE PRECAST INDUSTRIES IN TEXAS: TECHNICAL REPORT

by

Anol Mukhopadhyay
Senior Research Scientist
Texas A&M Transportation Institute

Kai-Wei Liu
Assistant Research Scientist
Texas A&M Transportation Institute

Mostafa Jalal
Graduate Student
Texas A&M Transportation Institute

and

Jia-Lin Hsu
Graduate Student
Texas A&M Transportation Institute

Report 5-6656-01-R1
Project 5-6656-01
Project Title: Verification of ASR Resistance Property of the Selected Concrete Mix Designs by the Precast Industries in Texas

Performed in cooperation with the
Texas Department of Transportation
and the
Federal Highway Administration

Published: September 2021

TEXAS A&M TRANSPORTATION INSTITUTE
College Station, Texas 77843-3135

DISCLAIMER

This research was performed in cooperation with the Texas Department of Transportation (TxDOT) and the Federal Highway Administration (FHWA). The contents of this report reflect the views of the authors, who are responsible for the facts and the accuracy of the data presented herein. The contents do not necessarily reflect the official view or policies of FHWA or TxDOT. This report does not constitute a standard, specification, or regulation. The research scientist in charge of the project was Dr. Anol K. Mukhopadhyay.

The United States Government and the State of Texas do not endorse products or manufacturers. Trade or manufacturers' names appear herein solely because they are considered essential to the object of this report.

ACKNOWLEDGMENTS

This project was completed in cooperation with TxDOT and FHWA. The authors wish to express their appreciation to TxDOT and FHWA personnel for their support throughout this study. Special thanks are extended to Darrin Jensen for serving as project coordinator. The research team highly appreciates the technical feedback provided by Andy Naranjo during the course of this project. Acknowledgment is also given to the staff at the Texas A&M Transportation Institute.

TABLE OF CONTENTS

LIST OF FIGURES

LIST OF TABLES

CHAPTER 1: INTRODUCTION

1.1 BACKGROUND AND SIGNIFICANCE OF WORK

The Texas Department of Transportation (TxDOT) has dedicated considerable resources to expanding the use of precast concrete in Texas bridges for decades [1, 2]. The use of precast panels eliminates the majority of formwork for concrete bridges, decreases construction time, and reduces construction costs [3]. However, alkali-silica reaction (ASR) has been identified in precast bridge structures (e.g., moderate cracking in precast girders) and is widespread throughout North America [4].

TxDOT has applied several measures step-wise since 1999 to control ASR in concrete structures. Although the recommendation in 2014 [5] was to use one of the five design options (Option 1: 20–35 percent of Class F fly ash; Option 2: 35–50 percent of slag or modified Class F ash [MFFA]; Option 3: 35–50 percent of a combination of Class F ash [≤ 35 percent] ± slag ± MFFA ± ultrafine fly ash [UFFA] ± metakaolin ± silica fume [≤ 10 percent]; Option 4: different cement types [type IP, IS, or IT] for different classes of concrete; Option 5: 35–50 percent of a combination of Class C fly ash [≤ 35 percent] ± silica fume [≤ 10 percent] ± UFFA ± metakaolin) to avoid ASR distress in precast concrete, replacing 25 percent of cement with Class F fly ash (Option 1) was applied to all precast concrete [2, 6]. It was observed that optimum fly ash content actually depends on aggregate reactivity, aggregate ASR threshold alkalinity (THA), and fly ash characteristics (e.g., CaO percent, soluble alkalis, glass composition and content) [7]. Therefore, assigning a common fly ash replacement level irrespective of these factors (i.e., one size fits all) may not be adequate.

In previous research projects, 0-6656 [8] and 0-6656-01 [9], an approach to design an ASR-resistant concrete mix based on composite activation parameter (CAP), THA, pore solution alkalinity (PSA), and concrete validation testing using the accelerated concrete cylinder test (ACCT) was developed and validated. The procedure to formulate ASR-resistant concrete mixes involves four steps:

- Step 1: Determination of CAP and THA using a volumetric change measuring device (VCMD)-based aggregate-solution test.
- Step 2: Formulation of an ASR-resistant mix by applying mix design controls depending on CAP-based reactivity prediction, THA, and some consideration of the severity of ambient conditions. Guidelines on selecting suitable mix design controls have been developed.
- Step 3: Mix design adjustment/verification based on the THA-PSA relationship (e.g., PSA needs to be below THA to prevent/minimize ASR) performed as an optional control.
- Step 4: Mix design validation through concrete testing—use of ACCT method to measure expansion of concrete cylinder in a short time.

Guidelines on different options for formulating ASR-resistant concrete mixes based on utilization of the four steps and depending on the needs related to testing duration and reliability were also developed and are summarized in Table 1.

Table 1. Different Options for Formulation of ASR-Resistant Mixes.

Option	Recommendation on Utilization of Step(s)/Method	Test Duration	Reliability	Outcomes
I	Use of all four steps	~ 2–3 months	Highest	Determination of CAP and THA using the VCMD method (Step 1) and formulation of ASR-resistant job concrete mixes (Step 2) followed by mix design verification using Step 3 and validation using the ACCT method (Step 4).
II	Use of Steps 1 to 3	≤ 20 days	Medium	Determination of CAP and THA using the VCMD method (Step 1) and formulation of ASR-resistant job concrete mixes (Step 2) followed by mix design verification using Step 3 (high importance) with no need for concrete validation testing (Step 4).
III	Use of the ACCT method to measure aggregate reactivity (like ASTM C1293)	28–45 days	High-Higher	Determination of aggregate reactivity using the ACCT method with lower level of alkali loading (i.e., 4.5 lb/cy) followed by mix design formulation using current practices (AASHTO R80-17/ASTM C1778).
IV	Use of the ACCT method to test job concrete mix (Step 4) formulated based on current practices	45–75 days	Medium-High	Formulation of job concrete mixes based on either mix design options (Options 1–6) in the TxDOT specification or in accordance with AASHTO R80-17/ASTM C1778 and validated using the ACCT method.

1.2 RESEARCH OBJECTIVES

The main objectives of this study were to verify the ASR resistance property of the selected concrete mix designs of bridge girders by the precast producers (PCPs) in Texas by applying the combined approach (Option I in Table 1) developed in Research Projects 0-6656 and 0-6656-01. The specific objectives were as follows:

- Use the VCMD method to test the aggregates and to measure ASR reactivity in terms of measuring CAP using American Association of State Highway and Transportation Officials (AASHTO) 364-17 and THA. Determine alkali loading by converting the THA using the calibration curve developed in Research Project 0-6656-01.
- Determine the reactivity of the studied aggregates with greater reliability. Determine reactivity using the ACCT method (Option III in Table 1) for all the selected aggregates as an alternative method and compare reactivity prediction by the three methods (i.e.,

VCMD method, ACCT method, and ASTM C1260-based reactivity data obtained from TxDOT) to ensure reactivity prediction with greater reliability.

- Establish an easy procedure to determine PSA for each mix from the selected PCPs. Both measurement of PSA using the conventional extraction technique and estimation of PSA using a new technique developed by the researchers (i.e., cement PSA by the National Institute of Standards and Technology [NIST] model + fly ash available alkalis by the ASTM C311 method) were proposed. Identification and quantification of alkali-contributing crystalline phases by the quantitative X-ray diffractometry (QXRD) method was proposed to check the reliability of available alkalis measured by ASTM C311 for the studied fly ashes and validation of the approach developed for PSA estimation.
- Reproduce the selected precast mixes in the lab and test using the ACCT method to determine if the mixes are adequate to prevent ASR or need some adjustments (e.g., changing the fly ash replacement levels).

1.3 ORGANIZATION OF THE REPORT

The work that was performed under different tasks (according to the original proposal) is presented in this report as chapters. The project's Value of Implementation (VoI) based on the development of the qualitative and economic benefit areas is determined and shown in Appendix B.

- Chapter 1 is an introduction describing the research background and objectives, as well as the report organization.
- Chapter 2 presents the material selection and collection from precast industries in Texas, followed by material characterization.
- Chapter 3 presents a detailed testing plan including determination of concrete threshold alkali loading and verification of different options (different combinations of the four steps depending on the need for rapidity [shorter testing period] and reliability) for the precast concrete mix design.
- Chapter 4 provides a summary and conclusions based on the findings from this study and recommendations for additional implementation work.

CHAPTER 2: MATERIALS

This chapter presents the material selection and collection from the selected PCPs in Texas, followed by a discussion of relevant material characterization. The obtained information from the selected PCPs pertaining to their current mix design practices included types of aggregates (if ASR reactive, then reactivity information was based on the current ASR test methods), fly ash type and replacement levels, and types of mixes.

2.1 MATERIAL SELECTION AND COLLECTION

Researchers proposed that at least two PCPs should be selected. All the potential PCPs were identified after critically analyzing the existing ASR data and obtaining feedback from the project manager and technical committee members. Based on the information collected, three out of five major PCPs in Texas were selected and contacted. The selected concrete mix designs along with the type and source of aggregates, supplementary cementitious materials (SCMs), and cement and chemical admixtures (e.g., high range water reducers [HRWRs], retarder, modifier) from these PCPs were collected. From each PCP, the required quantities of both coarse and fine aggregate, fly ash, cement, and admixtures were collected to reproduce these precast concrete mixes in the lab (Chapter 3).

The collected concrete ingredients from each PCP contained around 45 gal of both coarse and fine aggregate, 4 gal of both cement and fly ash, and 16 oz of varying admixtures used in the mix design. A summary of the detailed mix design information along with available aggregate reactivity data (ASTM C1260) of the three selected PCPs is provided in Table 2.

Table 2. Selected Concrete Mix Designs of Precast Industries in Texas.

Producer	PCP1	PCP2	PCP3
Coarse aggregate, 14 days C1260 expansion, %	0.008	0.031	0.179
Fine aggregate, 14 days C1260 expansion, %	0.231	0.141	0.302
Cement type	Type III	Type III	Type III
w/cm ratio	0.353	0.36	0.323
Coarse aggregate factor	0.58	0.72	0.61
Cement factor, sacks/cy	7.98	7.98	7.98
Fly ash, %	20% Class F	20% Class F	20% Class F
Air factor, %	2	1.5	2
HRWR, ounce/100lb	5.5	7	6.7
Retarder, ounce/100lb	3	0.5	1
Viscosity modifier, ounce/100lb	1	3.5	—
Corrosion inhibitor	—	51	—

According to Table 2, the selected PCPs use alkali-silica reactive aggregates with varying ranges of aggregate reactivity (i.e., reactive fine aggregate with PCP1 and PCP2, both reactive fine and coarse aggregates with PCP3). It seems that one of the current practices PCPs use to prevent ASR is to reduce concrete alkali loading by replacing cement with 20 percent Class F ash. However, based on the results obtained from the previous project (0-6656-01), the current practice of using TxDOT Option 1 with 20–35 percent Class F ash is safe for aggregates with alkali loading requirements of ≥ 3.6 lb/cy. Verification of the ASR resistance property of these mixes is provided in Chapter 3.

2.2 MATERIAL CHARACTERIZATION

For each PCP, the aggregate properties including, but not limited to, dry-rodded unit weight (DRUW), absorption capacity (AC) percent, and specific gravity for the collected aggregates were determined and the reactive constituents in the aggregates were identified via petrographic examination (ASTM C295). The bulk chemical analysis of the cement and fly ashes was determined using an X-ray fluorescence (XRF) device. The identification and quantification of crystalline phases in the selected cement and fly ash samples and amorphous content in fly ashes were determined via X-ray diffraction (XRD). The particle size distribution (PSD) for the selected cements and fly ashes was determined by a laser particle size distribution (Horiba LA-960).

2.2.1 Aggregate Properties

All aggregate-related properties (e.g., DRUW, specific gravity [SG_{od}], and AC percent) were determined and are presented in Table 3. The DRUW, AC percent, and SG_{od} were measured according to ASTM C127, C128, and C138, respectively. The types of reactive constituents were identified in accordance with ASTM C295. These aggregate properties were used in the VCMD test to determine aggregate quantity and other parameters. It has been established in the previous research that the use of the ACCT method with relatively low alkali loading (i.e., 4.5 lb/cy without any alkali boosting) was effective for determining aggregate reactivity in a relatively short time (e.g., within 45 days) and showed a favorable comparison with ASTM C1293. Since there are no available ASTM C1293 aggregate reactivity data for the aggregates from the selected PCPs, the ACCT measurement was conducted to predict aggregate alkali-silica reactivity (Option III in Table 1), and the reactivity results are presented in Table 3. The detailed photomicrographs of the reactive constituents for each aggregate are shown and discussed in Appendix A.

Table 3. Properties of the Selected Aggregates.

Aggregate	DRUW, lb/ft^3	AC, %	SG_{od}	45-day ACCT, %	Types of Reactive Constituents
PCP1-FA	109.3	0.9	2.58	0.080 (MR)	Strained quartz and chert particles
PCP1-CA	102.2	0.7	2.76	0.007	A few cryptocrystalline quartz inclusions within limestone particles can be reactive
PCP2-FA	104.4	0.7	2.6	0.040 (MR)	Strained quartz and chert particles
PCP2-CA	99.7	0.8	2.55	0.020	Mainly chert particles with a few strained quartz particles
PCP3-FA	99.1	0.76	2.62	0.092 (MR)	Chert, chalcedony, strained quartz
PCP3-CA	100.63	1.9	2.55	0.041 (MR)	Chert particles with cryptocrystalline quartz and a few strained quartz particles

Note: FA: fine aggregate; CA: coarse aggregate; MR: moderately reactive/slow reactive.

Aggregates containing strained quartz and chalcedony are susceptible to alkali attack due to poor crystal structure. If the aggregates contain microcrystalline quartz/chert inclusions within a matrix made of mainly non-reactive phases, they are considered slow/late reactive aggregates [10]. In general, aggregates that show high 45-day ACCT expansion generally contain more than one reactive constituent (e.g., silica minerals with poor crystalline structure [e.g., chert with chalcedony], strained quartz). The presence of chert particles with a few strained quartz particles was observed in PCP2-CA. However, this coarse aggregate was passed using the ACCT method. It has been observed that the reactivity of chert particles varies depending on grain size (e.g., micro-crystalline to crypto-crystalline), texture and type of siliceous components. It seems PCP2-CA is a very slowly reactive aggregate. Therefore, extending the testing time (more than the normal recommended time) during determination of aggregate reactivity as well as testing the ASR-resistant property of the precast job mixes containing this aggregate is recommended.

2.2.2 Properties of Cement and Fly Ash

2.2.2.1 Cement Property

ASTM C150M specifies compositional requirements covering five major types of commercial Portland cement, namely Types I, II, III, IV, and V. All cements from the selected PCPs were Type III (Table 2). The chemical analysis of the collected cements is listed in Table 4.

Table 4. Chemical Properties of Cement.

Cement	PCP1	PCP2	PCP3
Chemical Composition (wt %)			
SiO_2, %	19.8	19.8	19.6
Al_2O_3, %	5.5	4.6	4.5
Fe_2O_3, %	2.0	3.2	3.1
CaO, %	63	64.5	65
MgO, %	1.2	0.7	0.7
SO_3, %	5.0	3.9	3.7
Na_2O, %	0.12	0.05	0.06
K_2O, %	0.44	0.77	0.78
Na_2O_e, %	0.41	0.55	0.56
Phase Content, %			
Alite C_3S	51.9	65.5	70.4
Belite C_2S	17.6	7.4	3.1
Aluminate C_3A	11.2	6.8	6.7
Ferrite C_4AF	6.1	9.7	9.4

The elemental oxide wt% of cement determined via XRF is used to estimate cement phase contents with the Bogue formulas. However, the Bogue method, being an indirect estimation technique, cannot accurately quantify the main cement phases, identify and quantify the sulfate phases, or determine the limestone and amorphous contents in cement. In order to accurately and directly quantify the cement phases to overcome the pitfalls of the Bogue method, the QXRD protocols developed in Research Project 0-6941 [11] were used, and the results are shown in Section 2.4.4.

2.2.2.2 Fly Ash Characterization

The chemical and physical properties of all the fly ashes from the selected PCPs were determined by ASTM C618/C311 procedures. The physical properties and chemical analysis along with the available alkali determined by ASTM C311 for the collected fly ashes are listed in Table 5.

Table 5. Chemical and Physical Properties of Fly Ashes.

Fly Ash	PCP1	PCP2	PCP3	ASTM C618 Limits	
Chemical Composition (mass %)				Class F	Class C
SiO_2, %	55.44	53.51	56.88		
Al_2O_3, %	20.59	18.41	20.71		
Fe_2O_3, %	4.94	5.09	4.45		
Sum of (SiO_2+Al_2O_3+Fe_2O_3)	79.97	77.01	82.04	70 min.	50 min.
CaO, %	12.34	14.14	10.57		
MgO, %	2.51	3.67	2.3		
SO_3, %	0.63	0.77	0.48	5 max.	5 max.
Na_2O, %	0.33	1	0.3		
K_2O, %	1.01	1.31	1.03		
Na_2O_e, %	0.99	1.86	0.98		
Moisture Content	0.05	0.05	0.09	3 max.	3 max.
Loss on Ignition	0.21	0.24	0.36	6 max.	6 max.
Physical Tests					
Fineness Retained on a 45-um sieve, % PSD, %	 27.29 16.50	 22.31 20.64	 29.29 25.65	 34 max.	 34 max.
Strength Activity Index (SAI) Ratio to Control @ 7 days	84	89	79	75 min.	75 min.
Water Requirement % of Control	95	95	95	105 max.	105 max.
ASTM C311					
Available Alkali Na_2Oe, %	0.37	0.52	0.32		

Based on the results presented in Table 5, all ashes meet the requirements of ASTM C618 for Class F ash. In general, SAI values show a positive correlation with the CaO (i.e., the higher the CaO, the higher the reactivity). However, the sum of SiO_2+Al_2O_3+Fe_2O_3 (SSAF) and SAI show a negative correlation (i.e., the higher the SSAF, the lower the SAI). This is an indication that a higher amount of SSAF in fly ash composition does not guarantee higher values in SAI. Therefore, it is not clear whether SAI and/or SSAF represent fly ash reactivity effectively. A comparison with QXRD data (i.e., amorphous contents and identification and quantification of crystalline phases) sheds some light on this aspect later in this report.

The available alkalis (AAK) of fly ash were estimated by ASTM C311 after 28 days of curing at 38°C. In general, Na_2O_e and CaO values of all the tested fly ashes show a good positive correlation with the AAK (i.e., the higher the Na_2O_e or CaO values, the higher the AAK). It seems the types and contents of crystalline phases (e.g., alkali sulfates such as arcanite and some specific Ca-bearing phases like anhydrite, free lime), along with some contribution from the amorphous phase in these ashes, control the AAK in these ashes. It can be inferred that the presence of these crystalline phases in these ashes (especially ash from PCP2) should be detected by QXRD, as further discussed in Section 2.2.4.

2.2.3 Laser Particle Size Analysis

A Horiba LA-960 laser particle size analyzer (PSA) was used to determine the PSD of the selected cements and fly ashes, and the results are presented in Figure 1 and Figure 2, respectively.

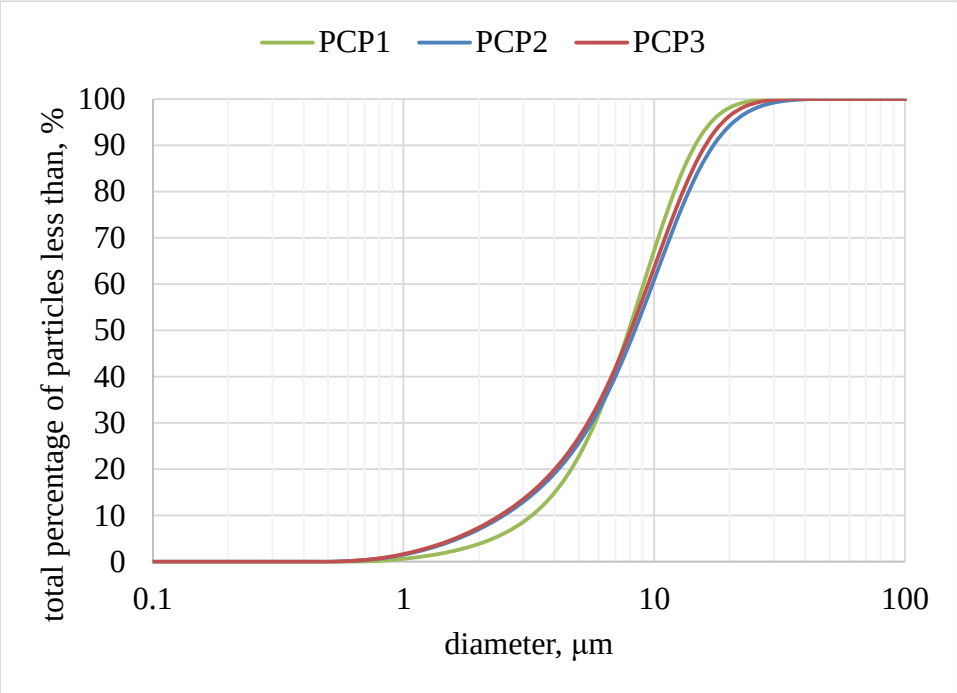

Figure 1. Particle Size Distribution of Cements.

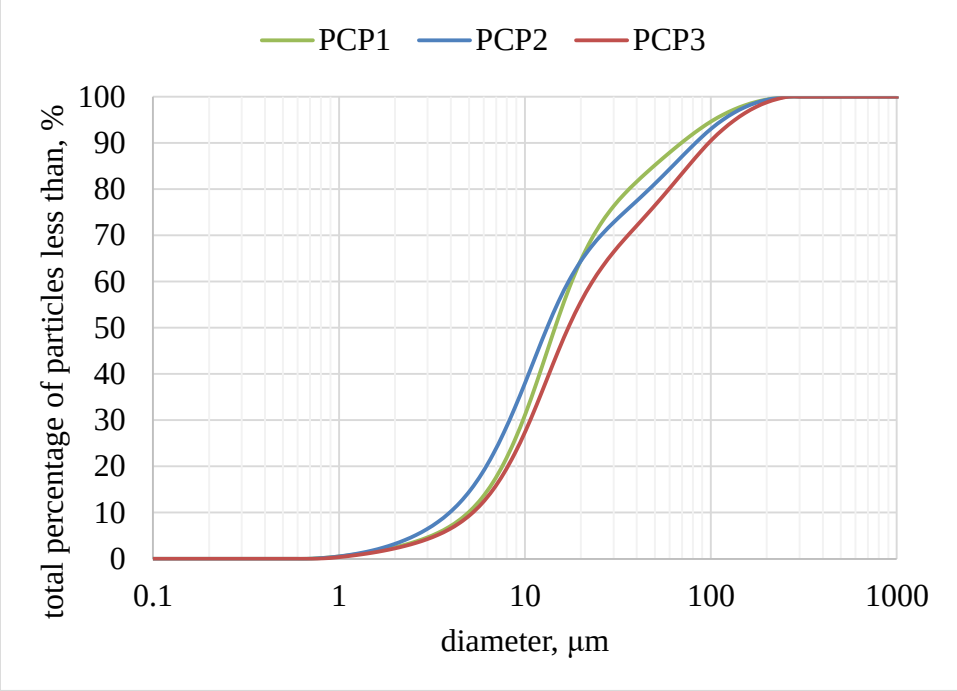

Figure 2. Particle Size Distribution of Fly Ashes.

Figure 1 shows all cements had similar medium particle size ranging from 7.9 to 8.4 μm. Figure 2 shows all fly ashes had medium particle size ranging from 13.1 to 17.2 μm with decreasing order as follows: PCP3 > PCP1 > PCP2. The fineness (residue on 45 μm sieve; see Table 5) results show a good positive correlation with the median size measured from the PSD. In general, the finer the ash, the higher the reactivity. However, pozzolanic reactivity of any fly ash can effectively be explained by a combined effect of its PSD, amorphous content and composition, and types and contents of specific crystalline phases. For example, fly ash from PCP2 shows the highest SAI, although PCP2 is slightly coarser than PCP1 and PCP3. The amorphous content determined by QXRD for these ashes, as discussed in the next section, provided a better explanation.

2.2.4 Quantitative X-Ray Diffraction

A Bruker D2 Phaser tabletop XRD with Cu Kα radiation was used to determine the amorphous content as well as identify and quantify the crystalline phases for the selected cements and fly ashes. Scans were run from 9 to 70 degrees 2θ for cement and 7 to 70 degrees 2θ for fly ash, with increments of 0.02 degrees and a counting time of 0.4 seconds per step. The identification and quantification of crystalline phases was performed using Rietveld refinement with the TOPAS 5.0 program. Amorphous content of fly ash was determined using the partially or not known crystal structures (PONKCS) method.

2.2.4.1 Phases in Cement

The cement samples received from all PCPs were analyzed via QXRD to identify and quantify crystalline phases such as alite, belite, aluminate, ferrite, and alkali sulfates (e.g., arcanite and thenardite). Table 6 illustrates the QXRD analysis of each cement from the selected PCPs. Alkali sulfates such as arcanite and thenardite were identified/quantified for the cements from PCP1 and PCP3, and syngenite was identified/quantified for the cement from PCP2. These alkali sulfates contribute soluble alkalis in concrete pore solutions. The cement from PCP2 might contribute a slightly higher range of soluble alkalis in the pore solution than cements from PCP1 and PCP3 because the PCP2 cement contains a more soluble syngenite ($K_2SO_4 \cdot CaSO_4 \cdot H_2O$) phase.

Table 6. QXRD Results for Cement.

Phases, wt%	PCP1	PCP2	PCP3
C_3S	53.6	60.0	62.9
C_2S	22.7	18.6	13.7
C_3A	9.3	3.9	4.3
C_4AF	6.0	9.9	10.6
Basanite	0.7	1.2	1.5
Gypsum	4.5	2.3	2.0
Syngenite	0.8	2.7	2.2
Thenardite* Na_2SO_4	1.1		0.9
Arcanite* K_2SO_4	1.1		0.8
Calcite		1.1	0.6
Lime		0.3	0.4
Dolomite			0.2

* Alkali sulfate.

2.2.4.2 Phases in Fly Ash

Identification and quantification of the crystalline phases and quantification of the amorphous (glassy) phase for the studied fly ashes were performed via XRD using TOPAS 5.0 software equipped with the Rietveld refinement method. Table 7 summarizes the phases present in the three fly ashes. The results show that the PCP1 ash contains more crystalline impurity (quartz) than the other ashes. The PCP2 ash shows the presence of crystalline phases such as alkali sulfates (arcanite) and Ca-bearing phases (e.g., free lime, alite, and akermenite). These crystalline phases (especially arcanite) seem directly related to the higher amount of available alkalis (0.52 percent) in the PCP2 ash. Moreover, a higher abundance of non-alkali-bearing sulfate phases (e.g., anhydrite) was observed in the PCP1 and PCP3 ashes than in the PCP1 ash. Therefore, identification and quantification of relevant crystalline phases via QXRD can effectively explain the soluble or available alkalis in fly ash but not the fly ash bulk alkalis (Table 5). Amorphous content (AMC) of the tested ashes with decreasing order is as follows: PCP3 > PCP1 > PCP2. AMC should be positively correlated with fly ash reactivity (e.g., SAI in Table 5). The SAI values for these ashes with decreasing order are as follows: PCP2 > PCP1 > PCP3. A poor positive correlation between AMC and SAI values was observed. Based on the earlier findings, SAI may not be an effective indicator of reactivity, so it is not unexpected to get this kind of poor correlation. Several researchers are pursuing studies to develop an effective way to measure fly ash reactivity (i.e., pozzolanic reaction/index). A good correlation between AMC and such an index (pozzolanic index) can become the basis for validating and recommending either AMC or pozzolanic index tests as a direct way to measure fly ash reactivity.

Table 7. QXRD Results for Fly Ash.

Phases, wt%	PCP1	PCP2	PCP3
Amorphous	67.76	61.60	68.18
Quartz	20.51	17.51	19.91
Anhydrite	0.32		0.42
Hematite	0.59	0.57	0.63
Merwinite $Ca_3Mg(SiO_4)_2$		2.03	
Mullite	10.68	7.38	10.59
Periclase	0.13		
Alite		7.88	
Free Lime		1.09	0.27
Arcanite* K_2SO_4		1.17	
Akermanite $Ca_2MgSi_2O_7$		0.44	

* Alkali sulfate.

2.3 SUMMARY

Based on the results, the following conclusions can be drawn:

- ASTM C618 may be appropriate for evaluating the consistency and uniformity of fly ashes but may not be effective to predict their performance in concrete. It is not clear whether measurements of SAI and/or SSAF represent fly ash reactivity effectively.
- Identification and quantification of relevant crystalline phases via QXRD can effectively explain the soluble or available alkalis in fly ash. Establishing criteria based on amorphous content and composition can create a better representation of fly ash reactivity.
- The fly ash from PCP2 showed the presence of alkali sulfates (arcanite) and Ca-bearing phases (e.g., free lime, alite, and akermenite). These crystalline phases (especially arcanite) seem directly related to the higher amount of available alkalis (0.52 percent) determined by ASTM C311 in the PCP2 fly ash.

CHAPTER 3: VERIFICATION OF ASR RESISTANCE PROPERTY OF SELECTED CONCRETE MIX DESIGNS BY PRECAST INDUSTRIES IN TEXAS

The current practice for formulating ASR-resistant mixes is to assign a common alkali loading applicable for all concrete mixes in different applications (i.e., one size fits all). However, the most effective approach to designing an ASR-resistant mix relies on determining the alkali loading of individual aggregates. Current ASR test methods are not capable of determining THA and/or alkali loading of an aggregate. The objective of the work described in this chapter was to verify the ASR resistance property of the selected concrete mix designs from the precast industries in Texas by applying the approach developed in Research Projects 0-6656 and 0-6656-01. The selected mixes were tested using Option I (Steps 1 to 4, Table 1) listed in Chapter 1.

3.1 AGGREGATE TESTING USING THE VCMD METHOD

Table 8 presents the design of the experiments. The selected aggregates (i.e., both 45-day ACCT expansion ≥ 0.04 percent and 14-day ASTM C1260 ≥ 0.1 percent) were tested using the VCMD (AASHTO T364-17 [12]according to the experimental design described in Table 8, and ASR free volume change over time was measured at multiple temperatures and alkalinities. In the VCMD test, an as-received aggregate is immersed in a soak solution, and the solution volume change is measured through a float–linear variable differential transformer (LVDT) data acquisition system over time at three temperatures (e.g., 60, 70, and 80°C inside an oven) followed by calculation of rate constants at the three tested temperatures (T) and determination of CAP based on Arrhenius rate theory [8, 12, 13]. Extensive aggregate testing has shown that a representative CAP can be determined within 5 days and with permissible repeatability. Using an automatic data acquisition system, testing inside an oven to maintain the testing temperature in a closed environment, and using a fundamental engineering property (i.e., CAP) as a measure of aggregate reactivity increases the reliability of the VCMD test. The CAP for all the tested aggregates, along with ASTM C1260 and ACCT expansion (percent), is listed in Table 9. In general, CAP, ACCT, and C1260 show a good correlation (i.e., the higher the ACCT/C1260 expansion, the lower the CAP). Typically, ACCT, C1260, and CAP-based reactivity predictions provide similar aggregate reactivity classification. The aggregates mainly belong to the moderately reactive (MR) category. Some of the aggregates that belong to the MR category can be slowly reactive (SR), but ASTM C1778 does not provide an SR category. As a result, some of these MR aggregates may show lower expansion at the specified time (not matching with their MR nature) because of their slow reactive nature.

Table 8. Factors and Levels in the Design of Experiments.

Factors	No. of Levels	Level Description
Material Type	6 aggregates	Aggregates listed in Table 2
Temperature	3	60, 70, and 80°C
Solution Normality	2	0.5 N and 1 N NH with CH—CH is added until above saturation

Table 9. CAP Values for the Tested Aggregates at Two Levels of Alkalinities along with 14-Day C1260- and 45-Day ACCT-Based Reactivity Values.

Aggregate	C1260 Value	Aggregate Reactivity Based on C1260	ACCT Value	Aggregate Reactivity Based on ACCT	CAP, KJ/Mol		Aggregate Reactivity Based on CAP Classification at 0.5N NH + CH
					0.5 N NH + CH	1 N NH + CH	
PCP1-FA	0.231	MR	0.080	MR	40.1	32.0	HR
PCP1-CA	0.008	NR	0.007	NR	—	—	NR
PCP2-FA	0.141	MR	0.040	MR	48.3	25.2	MR
PCP2-CA	0.031	NR	0.020	NR	—	—	NR
PCP3-FA	0.302	HR	0.092	MR	39.9	19.5	HR
PCP3-CA	0.179	MR	0.041	MR	31.5	21.2	HR

Note: VHR: very highly reactive; MR: moderately reactive/slow reactive; HR: highly reactive/reactive; NR: nonreactive.

An apparent relationship between CAP and alkali concentration (e.g., alkalinity) is evident from the results of the studied aggregates (see Table 9). The higher the alkalinity, the lower the CAP. This possibly suggests that the energy barrier to initiate ASR becomes low at high alkalinity and high at low alkalinity. An attempt was made to establish a mathematical relationship between CAP and alkalinity via the following model (Equation 3.1):

$$CAP = \mathrm{E}_{a_0} + \frac{C_1}{C^n} \qquad \text{(Equation 3.1)}$$

Where CAP is the composite activation parameter (KJ/mol), E_{ao} is the activation parameter theoretical threshold (KJ/mol), C_1 is the activation parameter curvature coefficient (KJ/(mol)$^{1-n}$), n is the activation parameter curvature exponent, and C is alkalinity (mol).

By fitting the above equation to the measured CAP and solution alkalinity, the characteristic trend is obtained. The existence of a characteristic THA for each aggregate was manifested from the calculated trend between CAP and alkalinity. Figure 3 shows a typical trend of that relationship (the green line) for an aggregate. Based on many tests, it was found that the point with a slope of −100 on a defined trendline (for example, the green line in Figure 3) effectively represents the THA (for example, the blue star in Figure 3) of the tested aggregate. A THA for each aggregate is summarized in Table 10. The THA is a very useful parameter to determine permissible concrete alkali loading for different aggregate sources. Pore solution alkalinity of different concrete mixes covering low to high alkali loadings was determined by using the pore solution extraction techniques and a linear relationship with high R^2 between PSA (normality) and alkali loadings was developed in Research Project 0-6656-01. This linear equation (lb/cy = 5.26 × normality + 1.26) was used to covert the measured THA (normality) to threshold alkali loading (TAL, in lb/cy, Table 10). A reactive aggregate can practically behave as nonreactive or very slow reactive if concrete alkali loading remains below TAL. The VCMD method has the merit to be used as an alternative to the ASTM C1260. However, the user can select any suitable rapid and reliable method to determine aggregate reactivity and THA.

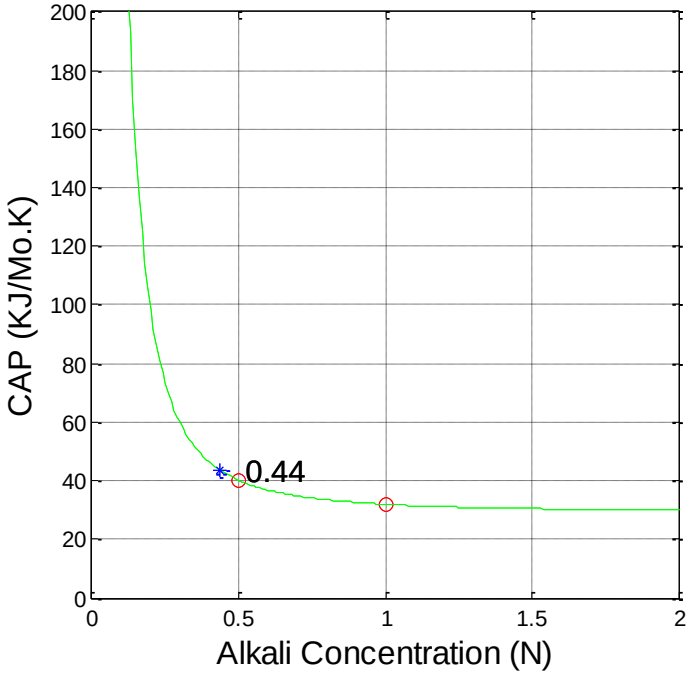

Figure 3. Example of THA Determination of the PCP1-FA Aggregate.

The red circles are plots of the measured CAP values at 0.5 and 1 N solutions. The blue star is the calculated THA value.

Table 10. Summary of THA.

Aggregate	C1260 Value	ACCT Value	THA N	TAL lb/cy	Aggregate Reactivity Based on the ACCT Method
PCP1-FA	0.231	0.080	0.44	3.6	MR
PCP1-CA	0.008	0.007	—	—	NR
PCP2-FA	0.141	0.040	0.49	3.9	MR
PCP2-CA	0.031	0.020	—	—	NR
PCP3-FA	0.302	0.092	0.46	3.7	MR
PCP3-CA	0.179	0.041	0.45	3.6	MR

3.2 VERIFICATION OF THE MIX DESIGNS

In order to verify the current mix design practices of the selected PCPs for ASR resistance, concrete mixtures were reproduced in the lab. The relationship between PSA and aggregate THA was used to predict the ASR potential of the studied precast concrete mixtures before conducting ACCT testing. If the PSA is lower than the THA, then the current mix design should be adequate to control ASR. However, if the PSA is higher than the THA, the current concrete mixture is not safe, and suggestions will be made to adjust (i.e., fine tune) these mixes to make them ASR resistant.

For PSA determination, the cement paste (cement + fly ash) cylinders (2 by 4 inches) matching with volumetric ratios of cement: fly ash: water corresponding to each concrete mix were cast and covered with plastic lid, and then cured under 98±2 percent relative humidity (RH) at 23±2°C for 7 days followed by de-molding and pore solution extraction by using a high-pressure squeezing method. Pore solution extraction from a minimum of three cement paste specimens followed by mixing of the extracted solution was completed for each mix to get a representative and suitable quantity of pore solution. The Na^+ and K^+ concentrations of the extracted pore solutions for each mix were determined using an XRF. It is recommended that PSA ($Na^+e = Na^+ + 0.59*K^+$) be determined based on the extraction technique since some fly ashes contribute soluble alkalis in the pore solution. If the pore solution extraction method is not available, use of the NIST predictive model combined with measurement of available alkalis via ASTM C311 is proposed. The proposed combined use of the NIST model and ASTM C311 to estimate PSA was validated previously by establishing a favorable comparison between PSA determined with the extraction technique and the proposed combined approach using fly ash from all PCPs [14].

PSA values measured using the extraction technique and estimated via the proposed combined approach (i.e., NIST model + ASTM C311) for all ashes are presented in Table 11. The explanation on how to estimate PSA based on the combined approach is provided through the following examples. For example, for PCP1 with a 20 percent fly ash replacement (FAR) level, the NIST model was used to estimate the PSA (0.11M Na^+ and 0.27M K^+) corresponding to 80 percent cement. The ASTM C311-based available alkali for fly ash was 0.03M Na^+ and 0.07M K^+. The estimated final PSA (i.e., 0.14M Na^+ and 0.34M K^+) was calculated by adding Na^+ and K^+ concentrations in the estimated pore solutions using the NIST model (cement portion) and in the available alkalis based on ASTM C311 (fly ash). The estimated PSA using the proposed combined approach (9th and 10th columns, Table 11) matches well with the measured PSA from the extraction technique (4th and 5th columns, Table 11) for all the fly ashes, which validates the applicability of the combined approach to estimate PSA of a cement-fly ash combination with acceptable accuracy. Interestingly, the estimated PSA based on the NIST model alone for each mix (7th and 8th columns) showed higher concentrations of both Na^+ and K^+ than those based on the extraction technique as well as the proposed combined approach. This is an indication of overestimation of PSA by the NIST model for cement-fly ash combinations.

Table 11. Pore Solution Chemistry Data of Mixes with Fly Ashes.

Fly Ash	FAR (%)	Alkali Loading (lb/cy) / THA(N)	Extraction (M)			NIST (M)		NIST (cement alone) + Available Alkali (ASTM C311) (M)		
			Na^+	K^+	Na_2O_e	Na^+	K^+	Na^+	K^+	Na^+_e
PCP1	20	2.5 / 0.44	0.12	0.37	0.34	0.23	0.52	0.11 + 0.03 = 0.14	0.27 + 0.07 = 0.34	0.34
PCP2	20	3.4 / 0.49	0.11	0.57	0.45	0.33	0.79	0.05 + 0.05 = 0.1	0.46 + 0.09 = 0.55	0.42
PCP3	20	3.4 / 0.45-0.46	0.1	0.59	0.45	0.19	0.95	0.07 + 0.02 = 0.09	0.57 + 0.06 = 0.63	0.46

An attempt has been made to predict ASR potential of the studied concrete mixes based on THA-PSA relationships. For example, expansion below the limit (0.04 percent) was predicted

for the PCP1 and PCP2 mixes as the relationship PSA < THA is clear for these mixes (e.g., PSA – 0.34 < THA – 0.44 for PCP1 and PSA – 0.45 < THA – 0.49 for PCP2). Therefore, these two mixes should be identified as safe mixes by the ACCT method. For the PCP3 mix, the PSA is slightly lower than the THA for the fine aggregate (0.46) but equal to the THA for the coarse aggregate (0.45). As a result, it is expected that the ACCT expansion should remain below the limit of 0.04% for the PCP3 mix, i.e., this mix should also be identified as safe mix.

3.3 CONCRETE TESTING USING THE ACCT METHOD

The ACCT method was previously developed based on a significant amount of research to assess alkali-silica reactivity of aggregates in concrete. A 3- by 6-inch concrete cylinder was placed inside the container after 7 days of curing in a moist room (RH @ 98±2 percent, temperature @ 23±2°C). The specimen was then immersed in a soak solution of chemistry equal to the PSA of the specimen. The LVDT was inserted through the center hole of the lid until it seated on the top surface of the concrete cylinder. Length change of the cylinder due to ASR expansion was recorded as LVDT displacements (inch) through the data acquisition [7, 9, 14-18].

The current test methods are not capable of detecting the effect of fly ash soluble alkali contribution in ASR expansion because these tests are conducted with alkali boosting conditions. It has been found that the ACCT method has the capability to detect this effect because the test is conducted without any alkali boosting. Moreover, the ACCT method with soak solution equal to pore solution best represents the field condition (i.e., a visualization of continuous supply of alkalis and moisture from the pore solution in the surrounding areas of a hypothetical concrete cylinder inside a field concrete structure matches well with the ACCT testing conditions). This eliminates alkali leaching and creates an alkali condition like field concrete.

The PCP concrete mix design details are presented in Table 2. Each concrete (Table 2) was mixed using the hand mixing procedures in accordance with ASTM C192. Two cylinders (3 × 6 inches) using each concrete mix were cast followed by curing periodically in a moist room (RH @ 98±2 percent, T @ 23±2°C) for 7 days.

All PCPs' concrete mixes listed in Table 2 were tested with the ACCT method. The ACCT method for each mix in Table 2 was conducted by immersing the specimen in a solution with alkalinity equal to the estimated (Table 11) PSA of that mix. As noted earlier, ACCT testing has the potential to detect the effects of soluble alkali contribution from fly ash on ASR expansion. Figure 4 to Figure 6 show the expansion curves over time for all the studied PCP mixes.

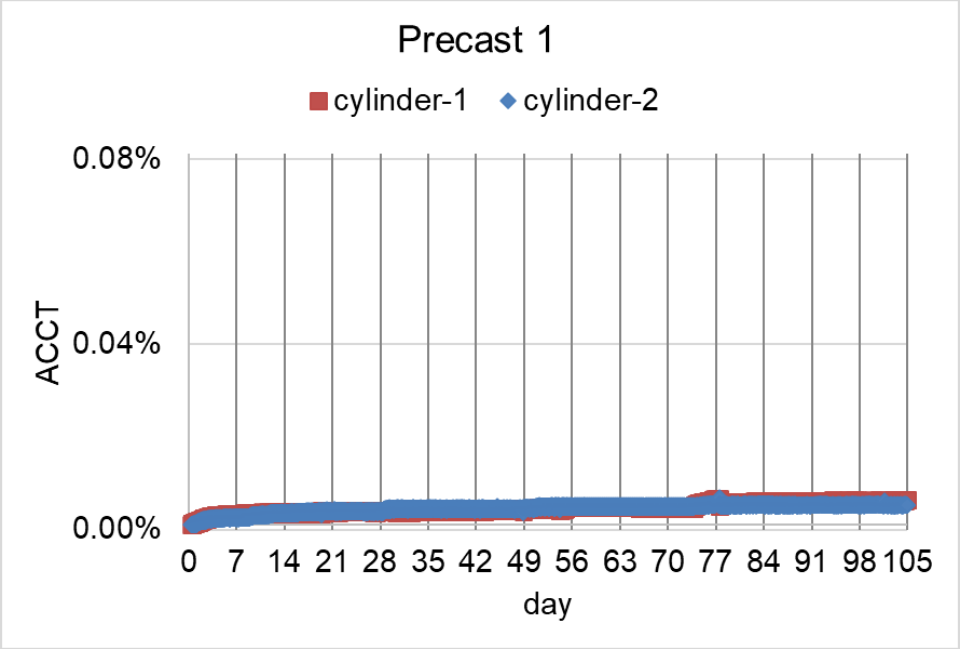

Figure 4. Expansion of Concrete Mix from PCP1.

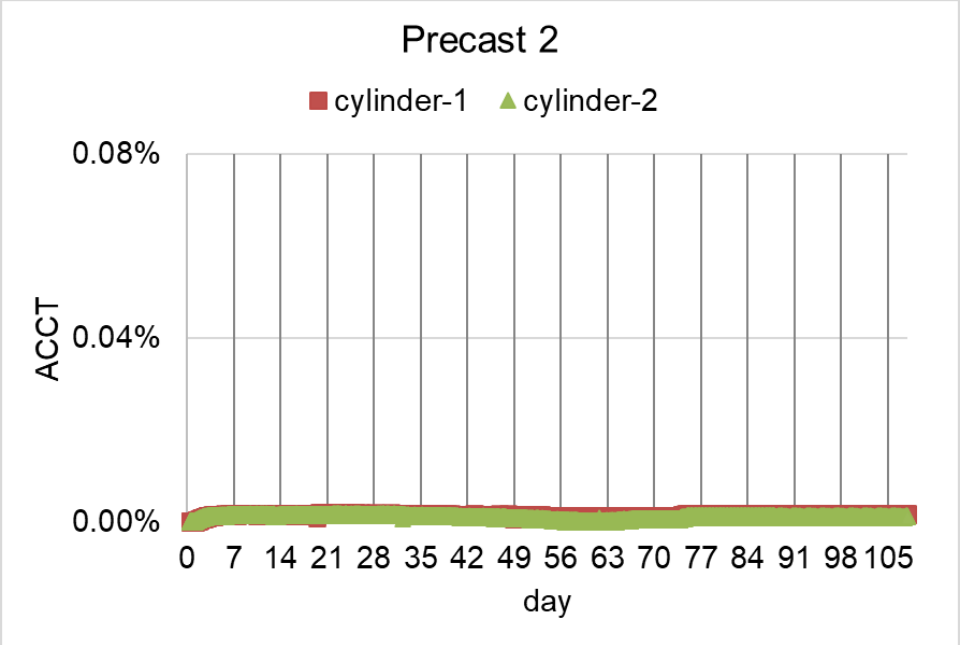

Figure 5. Expansion of Concrete Mix from PCP2.

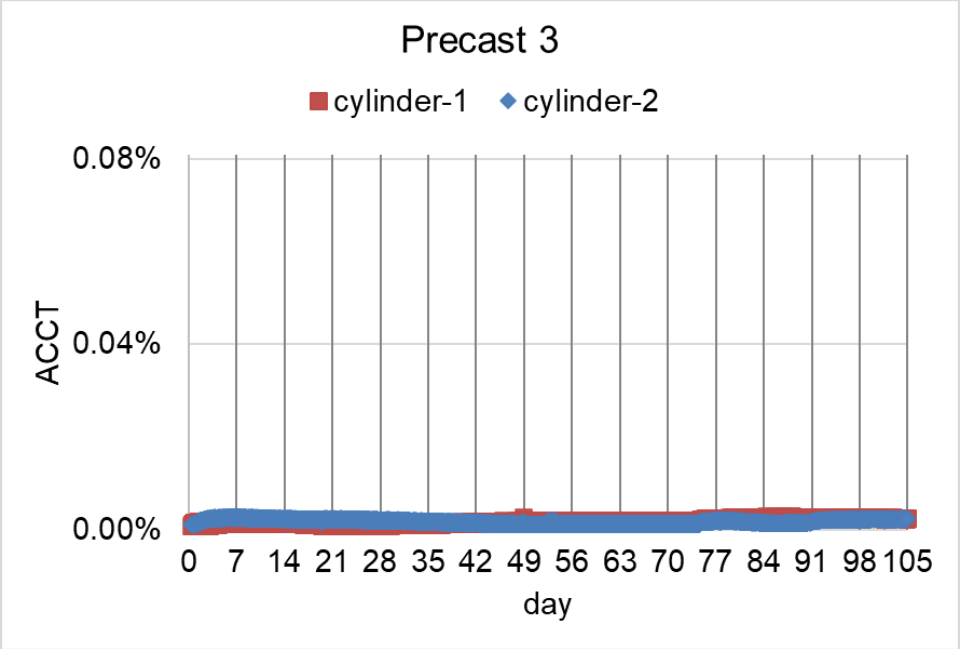

Figure 6. Expansion of Concrete Mix from PCP3.

Figure 4 to Figure 6 indicate that the predicted expansion based on the PSA-THA relationship (Section 3.2) is validated by the ACCT expansion data. The mix design controls (e.g., low w/c, low coarse aggregate factor [CAF], low cement alkali) and dense microstructures development may also have added some effects to prevent ASR expansion measured with the ACCT method. The studied precast job mixes are compared with the standard mixes used in the ACCT method in Table 12.

Table 12. Mix Designs of Earlier ACCT and PCP Job Mixes.

	w/c	CAF	Cement Alkali Na_2O_e, %	Cement Factor sack/cy	Fly Ash %	Alkali Loading lb/cy
PCP1	0.353	0.58	0.41	7.98	20	2.5
PCP2	0.36	0.72	0.55	7.98	20	3.4
PCP3	0.323	0.61	0.56	7.98	20	3.4
Earlier ACCT	0.45	0.76	0.82	5.83	0	4.5
					20	3.6
					25	3.4
					30	3.2
					35	2.9

In the ACCT measurement using standard mixes, the concrete mixes might have less-dense microstructures than the precast job mixes due to higher w/c (0.45) and lower cement factor (5.83), resulting in more movement of ions inside the concrete through the pore solution and penetration of ions from the soak solution at early ages. Thus, there is a chance to measure some expansion earlier by the ACCT testing using standard mixes compared to the precast job mixes. Due to the use of low w/cm (0.32–0.36) and high cement factor (e.g., 7.98) in the precast mixes and the relatively higher testing temperature (i.e., 60°C) of the ACCT method, the development of a denser concrete microstructure at early ages should occur.

The dense microstructural development of the precast concrete can affect ASR expansion in the following ways: (a) minimize ASR expansion (especially at the early ages) compared to standard concrete mixes due to a reduced rate of ionic movement (lesser degree of ASR) inside the concrete specimen as well as negligible penetration of soak solutions/ions from the soak solution into the specimen; and (b) enhance ASR due to relatively higher PSA because of the use of low w/cm, depending on the THA of the tested aggregate. In this situation, there is a possibility for some precast concrete to show relatively lower expansion than the standard mixes at the early ages (same age) and with the same alkali loading. Therefore, ACCT testing for these selected precast mixes was continued for a longer period (up to 105 days) to ensure a reliable verification.

3.4 SUMMARY

Based on the results, the following conclusions can be drawn:

- The combined use of the NIST model and ASTM C311 was found to be effective to estimate PSA of the concrete mix containing fly ash with acceptable accuracy and is recommended for use when the classical pore solution extraction method is not available.
- A comparative assessment between THA and PSA values allows predicting ASR potential of the studied precast mixes before conducting the ACCT-based concrete validation testing.
- The predicted expansion based on the PSA-THA relationship is validated by the ACCT expansion data. However, the microstructural differences between the standard ACCT mixes and precast job mixes may lead to creating cases such as some precast concrete mixes showing relatively lower expansion than standard ACCT mixes at the early ages (same age) and with the same alkali loading. Based on this possibility, continuation of the ACCT testing for a longer period (more than 75 days) is recommended to ensure reliable verification. As a result, ACCT testing for these selected precast mixes was continued for a longer period (up to 105 days) to ensure a reliable verification.

CHAPTER 4: CONCLUSIONS AND RECOMMENDATIONS FOR ADDITIONAL IMPLEMENTATION

This chapter summarizes the main findings of this study. Some additional implementation lab tests are also proposed.

4.1 CONCLUSIONS

Based on the results, the following conclusions are drawn:

- All the fly ashes used by the selected PCPs were determined to be good-quality Class F ashes. The relatively lower abundance of alkali sulfate phases determined by the QXRD method and lower available alkali measured by the ASTM C311 are the characteristics of these ashes, which are considered favorable factors for designing ASR-resistant mixes with relatively lower levels of replacement.
- Based on the earlier ACCT criteria (expansion limit of 0.04 percent @ 75 days), the selected PCP mix design with 20 percent FAR seems to be safe mixes. Due to the use of low w/cm (0.32–0.36) and high cement factor (e.g., 7.98) in the precast mixes and relatively higher testing temperature (i.e., 60°C) of the ACCT method, the development of a denser concrete microstructure at early ages should occur. The dense microstructural development of the precast concrete can minimize ASR expansion (especially at the early ages) compared to standard concrete mixes due to a reduced rate of ionic movement (lesser degree of ASR) inside the concrete specimen as well as negligible penetration of soak solutions/ions from the soak solution into the specimen. The relatively higher PSA in some precast mixes because of the use of low w/cm may enhance ASR depending on the THA of the tested aggregate. In this situation, there is a possibility for some precast concrete to show relatively lower expansion than the standard mixes at the early ages (same age) and with the same alkali loading. Therefore, continuation of the ACCT testing for a longer period (more than 75 days) is recommended to ensure reliable verification.
- A combined use of QXRD, PSD, and PSA data along with conventional ASTM C618 data was found to be very useful to predict fly ash performance and make recommendations on fly ash selection along with approximate level of replacement (lower or higher range at the best level) to prevent ASR in Portland cement concrete.
- The developed options listed in Table 1 allow TxDOT to successfully implement this approach for validation of PCPs' concrete mix design to prevent ASR. The approach can also enable producers and owners to formulate ASR-resistant mixtures using locally available aggregates, even in the event of shortages of Class F ash.

4.2 ADDITIONAL IMPLEMENTATION

Based on the results, the following additional implementations are recommended:

- As noted previously, there is a possibility for the precast mixes to show relatively lower expansion than the standard ACCT mixes at the early ages (same age) and with the same alkali loading, primarily because of the microstructural differences between the standard ACCT mixes and precast job mixes. In order to validate this

phenomenon, ACCT testing using both standard mixes and precast mixes (especially PCP3) with a 20 percent FAR level and a highly reactive fine aggregate is recommended.

- Extending the testing time for precast concrete mixtures using the ACCT method is recommended. Therefore, further long-duration testing is also recommended to determine the testing time for the PCP job mixes using the ACCT method.
- The current TxDOT practice to prevent ASR in precast concrete mainly relies on mix design Option 1 (i.e., 20–35 percent of Class F fly ash) with replacing 20 percent of cement with Class F fly ash. However, 20 percent Class F FAR level might not be sufficient to prevent ASR for all aggregates (especially the aggregates with higher reactivity and lower TAL) that are used to make precast concrete in Texas. The scarcity of Class F ashes is another concern. The information on types of aggregates used to make precast concrete in Texas by different PCPs along with their available reactivity data will be very useful. A reliable reactivity prediction of all these aggregates via the VCMD and ACCT methods and determination of their THA/TAL along with fly ash characterization using the innovative combined approach and PSA predictions will be useful to quickly predict the ASR potential of all selected precast mixes by different PCPs in Texas. Reproduction of all possible precast job mixes in Texas followed by direct validation via the ACCT method would be the best way to verify their ASR resistance property but doing so would take more time. Additional implementation using the developed and validated combined approach is needed to test different job concrete mixes containing different SCMs (e.g., Class C fly ashes, blended ashes, slags) to validate the ASR-resistant property of various concrete mix designs for different applications (e.g., cast-in-place bridge deck concrete and other substructure and superstructure concretes).
- Application of the QXRD method to determine glass content and crystalline phases that contribute soluble alkalis and sulfates for different types of SCMs (e.g., Class C ashes, off-spec blended ashes, ashes from blended coal, slags), along with pore solution measurement/estimation followed by ACCT testing, will be very useful for understanding the effectiveness of all available SCMs and their ability to reduce ASR.

REFERENCES

1. Medlock, R., M. Hyzak, and L. Wolf. *Innovative prefabrication in Texas bridges*. in *Proceedings of the Texas Section, ASCE, Spring Meeting*. 2002.
2. Bettis, G. *Expanding the Use of Precast Concrete in Texas Bridges*. 2013; Available from: https://ftp.dot.state.tx.us/pub/txdot-info/cst/conference/ca-10-graham-bettis.pdf.
3. Wood, S.L., *Recommendations for the use of precast deck panels at expansion joints*. 2008, University of Texas at Austin. Center for Transportation Research.
4. Thomas, M., et al., *Alkali-Silica Reactivity Field Identification Handbook*. 2011.
5. TxDOT, *Standard Specifications for Hydraulic Cement Concrete*, in *Item 421*. 2014, Texas Department of Transportation: Austin, Texas.
6. TxDOT, *Standard Specifications for Precast Concrete Structures (Fabrication)*, in *Item 424*. 2004, Texas Department of Transportation: Austin, Texas.
7. Mukhopadhyay, A.K. and K.-W. Liu, *Innovative Approach for Formulating ASR-Resistant Mixtures.* Concrete International, 2018. **40**(12): p. 39-45.
8. Mukhopadhyay, A.K. and K.-W. Liu, *ASR Testing: A New Approach to Aggregate Classification and Mix Design Verification*, in *No. FHWA/TX-14/0-6656-1*. 2014: Texas. Dept. of Transportation. Research and Technology Implementation Office.
9. Mukhopadhyay, A., K.-W. Liu, and M. Jalal, *Further Validation of ASR Testing and Approach for Formulating ASR-Resistant Concrete Mix: Technical Report*. 2018.
10. Gillott, J.E., M. Duncan, and E.G. Swenson, *Alkali-aggregate reaction in Nova Scotia IV. Character of the reaction.* Cement and Concrete Research, 1973. **3**(5): p. 521-535.
11. Mukhopadhyay, A., et al., *Direct Determination of Cement Composition by X-ray Diffraction*. 2019.
12. AASHTO, *T364-17 Determination of composite activation energy of aggregates due to alkali-silica reaction (chemical method)*. 2017, American Association of State Highway and Transportation Officials.
13. Liu, K.-W. and A.K. Mukhopadhyay, *A kinetic-based ASR aggregate classification system.* Construction and Building Materials, 2014. **68**: p. 525-534.
14. Mukhopadhyay, A., K.-W. Liu, and M. Jalal, *Performance based approach of fly ash characterization and optimization to prevent ASR.* ACI Structural and Materials Journals (in press), 2019.
15. Mukhopadhyay, A.K. and K.-W. Liu, *ASR testing: a new approach to aggregate classification and mix design verification: technical report*. 2014, Texas. Dept. of Transportation. Research and Technology Implementation Office.
16. Mukhopadhyay, A.K. and K.-W. Liu, *0-6656: ASR testing: a new approach to aggregate classification and mix design verification:[project summary]*. 2014, Texas. Dept. of Transportation.
17. Liu, K.-W. and A.K. Mukhopadhyay, *Accelerated Concrete-Cylinder Test for Alkali–Silica Reaction.* Journal of Testing and Evaluation, 2015. **44**(3): p. 1229-1238.
18. Mukhopadhyay, A.K. and K.-W. Liu. *Developing a Rapid Cylinder Test for Determination of Length Change of Concrete due to Alkali-Silica Reaction*. in *T95th Annual MeetingTransportation Research Board*. 2016.
19. TXDOT, *Report on Texas Bridges* 2018, Texas Department of Transportation: Texas.

APPENDIX A: PETROGRAPHIC OBSERVATIONS OF THE REACTIVE CONSTITUENTS FOR EACH AGGREGATE

Thin sections were prepared using representative aggregate samples by National Petrographic Services (NPS). These thin sections were observed under a transmitted light optical microscope to identify siliceous reactive constituents in the studied aggregates (ASTM C295). The description of the identified reactive constituents for each aggregate is presented below with representative photomicrographs:

PCP3-CA

This coarse aggregate sample mainly contains particles of chert, sandstone/metaquartzite, and few limestone particles. Presence of following reactive siliceous constituents was identified in this sample

- Chert particles with varying grain sizes (i.e., very fine to coarse grained) (Figure 7–Figure 9). Some particles show large grain size variation (coarse quartz to fine cryptocrystalline quartz, Figure 10) within a single particle. The reactivity of chert particles varies from slowly reactive to moderate depending on grain size (i.e., the finer the grain size, the higher the reactivity, in general).
- Sandstone/metaquartzite—next to chert in abundance. The presence of strained quartz (Figure 11) was observed in some metaquartzite particles. The strained quartz particles are ASR reactive with varying degrees depending on degree of strain effects.

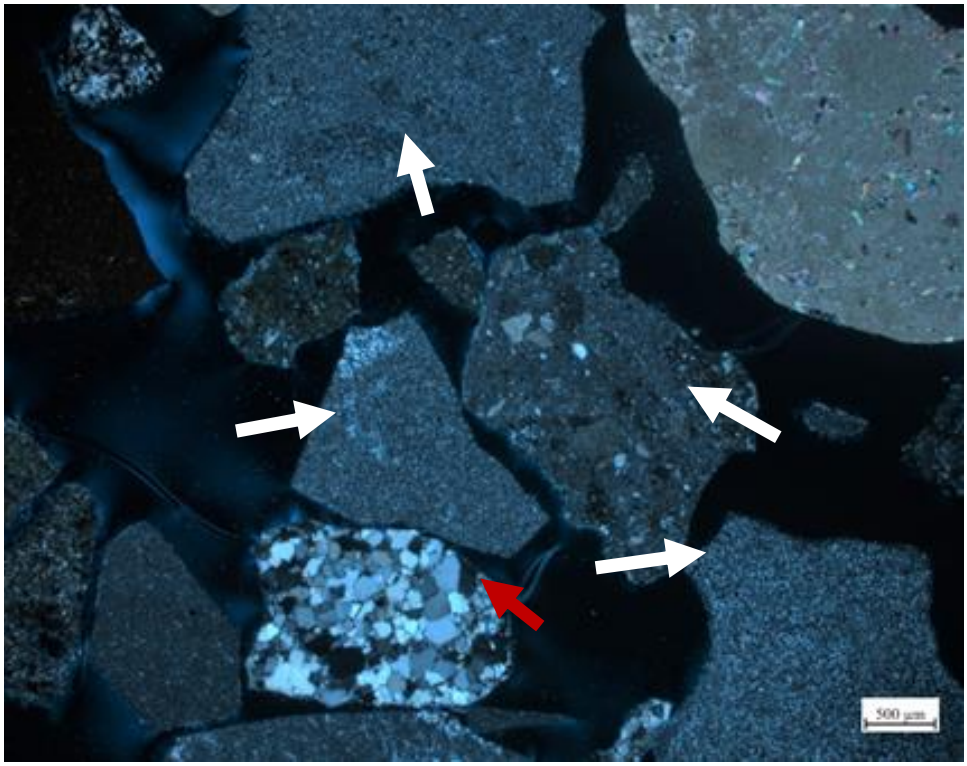

Figure 7. Chert Particles (White Arrows) along with a Few Quartzite Particles (Red Arrows), cross polarized light (XPL).

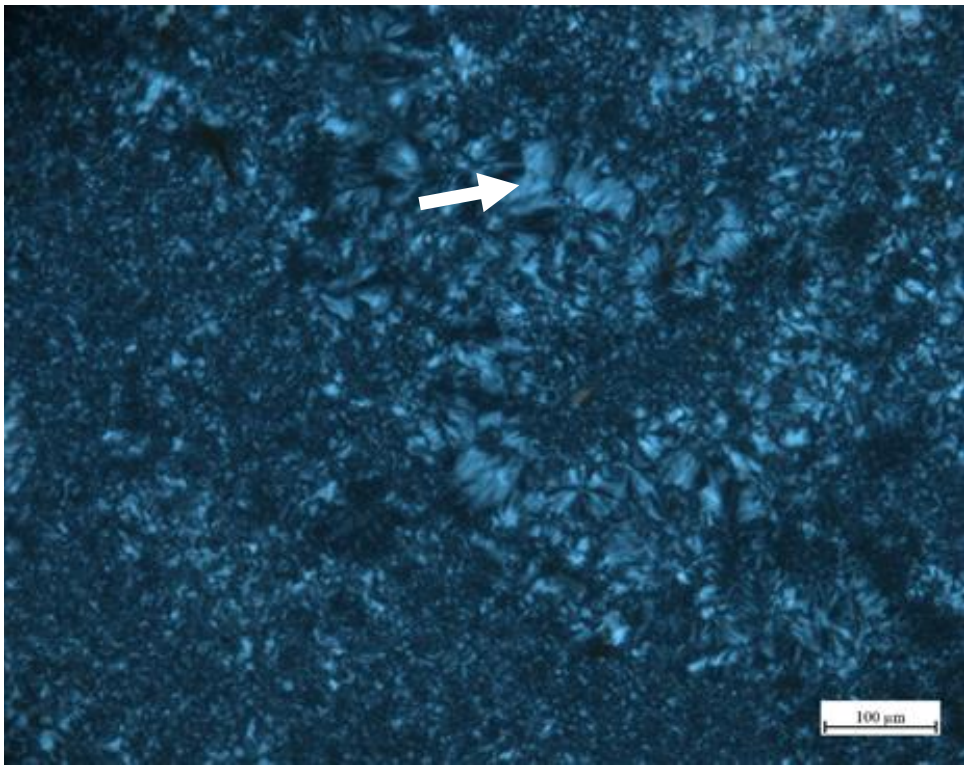

Figure 8. Fine-Grained Chert Made of Cryptocrystalline Quartz and Chalcedony (White Arrow), XPL.

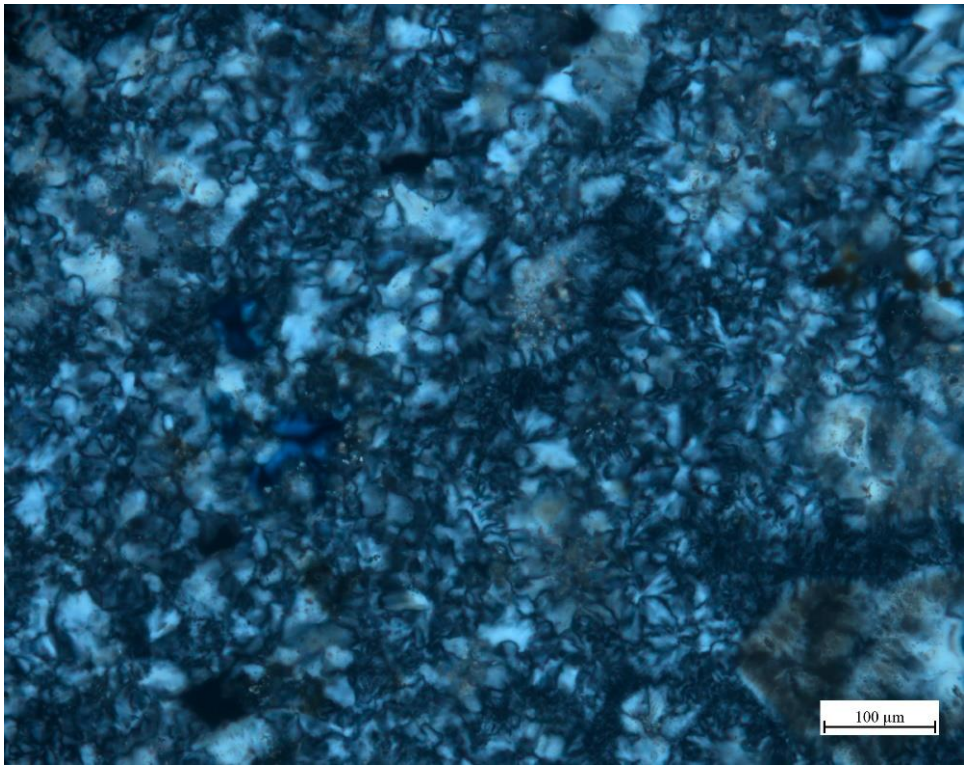

Figure 9. Relatively Coarse-Grained Chert Particles, XPL.

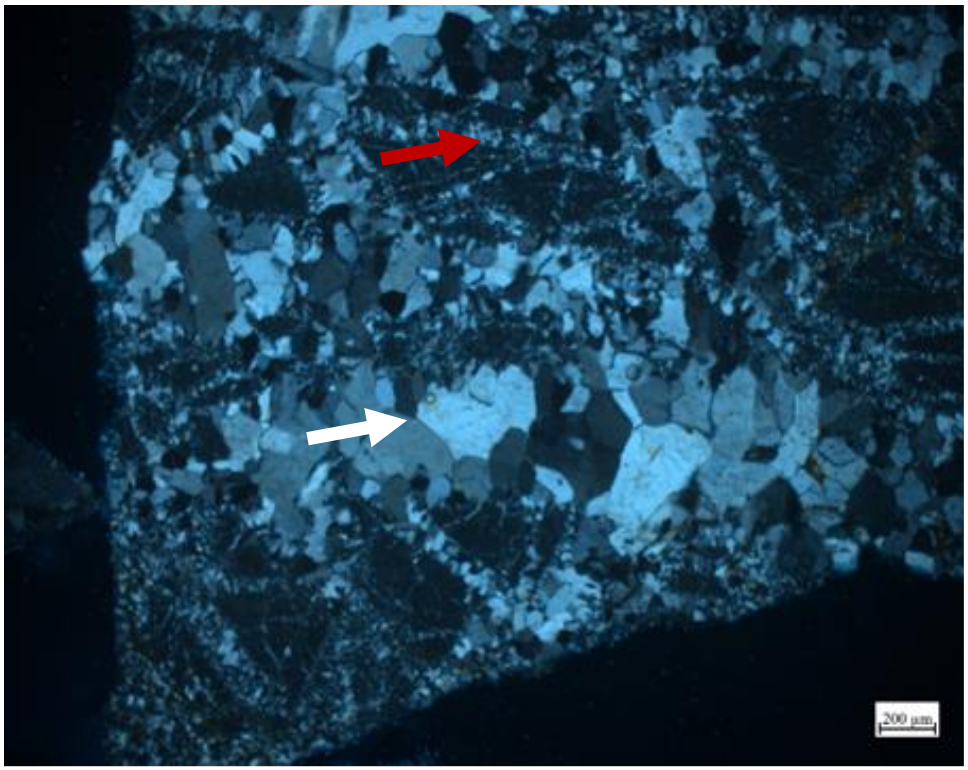

Figure 10. A Chert Particle Showing the Grain Size Variation (Coarse Quartz [White Arrow] to Fine Cryptocrystalline Quartz [Red Arrow]) within the particle, XPL.

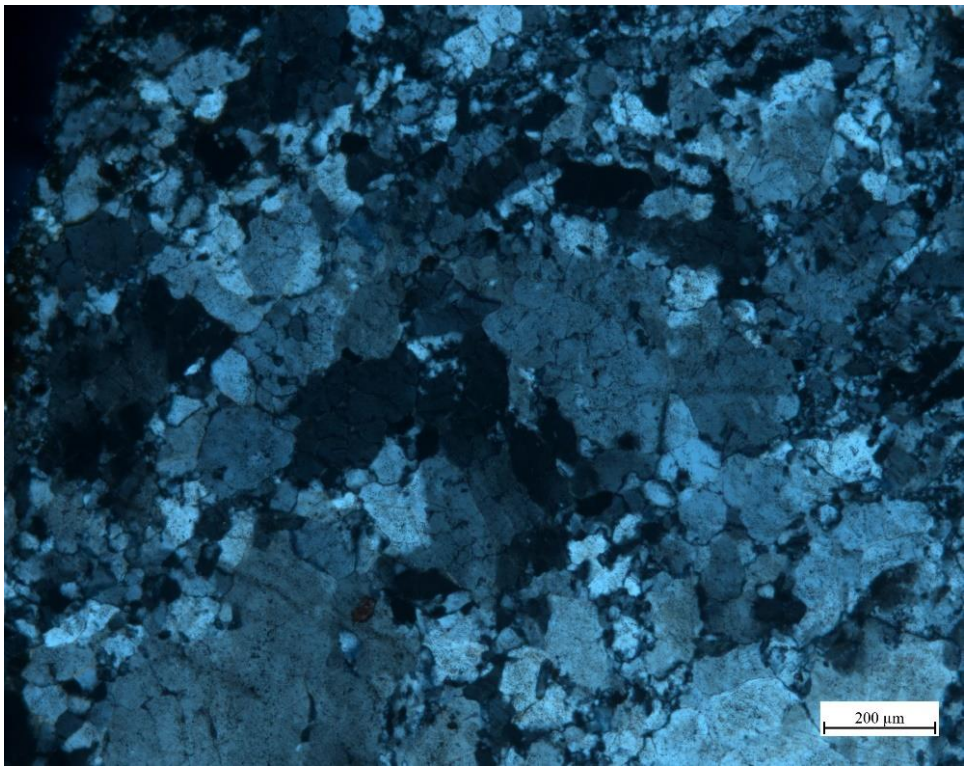

Figure 11. Appearance of Strained Quartz, XPL.

PCP2-FA

This fine aggregate sample contains quartz, feldspar, and chert particles (Figure 12) with Qtz >> feldspar ≥ chert in abundance.

- Chert particles (Figure 13) show variation in grain size (coarse to fine). The alkali-silica reactivity of chert particles varies depending on the grain size and texture.
- Quartz particles show undulate extinction with varying degrees (some do not show and some show very prominent strain effects, Figure 14). The quart grain with strain effects can be ASR reactive (slow or medium depending on degree of strain effects).

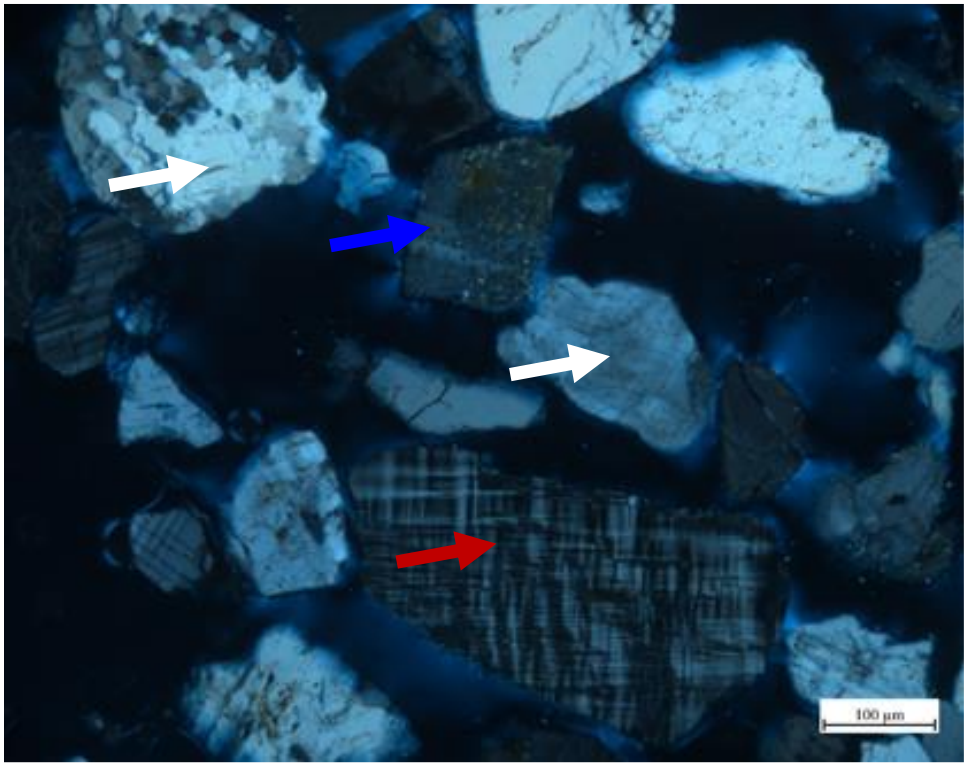

Figure 12. Feldspar (Red Arrow), Quartz (White Arrows), and Chert (Blue Arrow) Particles, XPL.

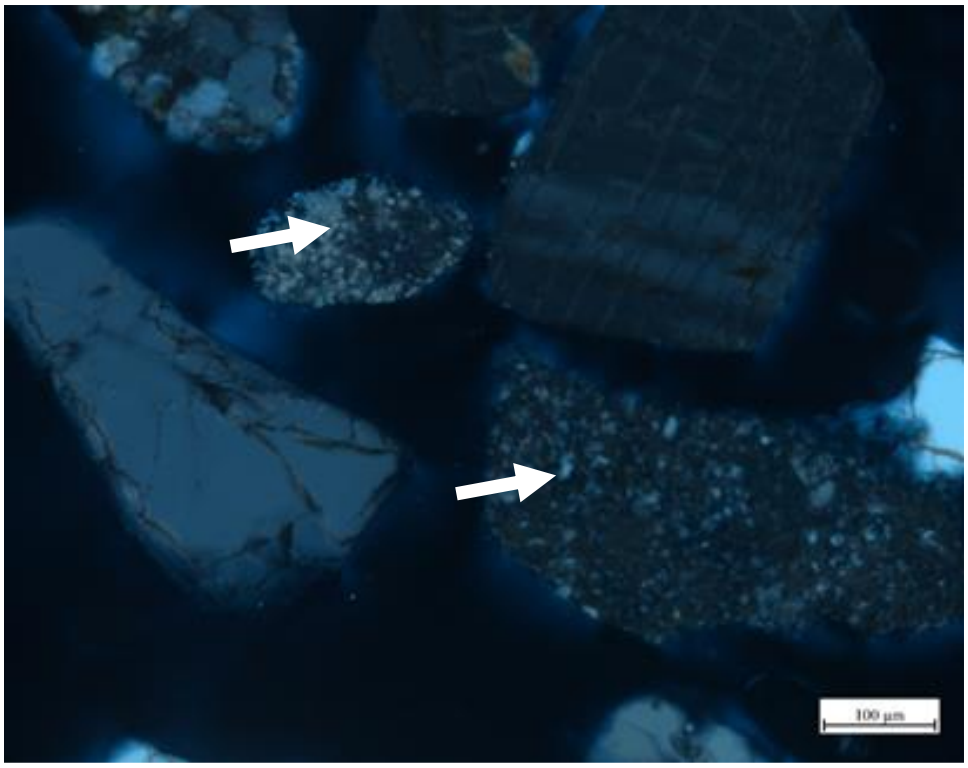

Figure 13. Chert Particles (White Arrows), XPL.

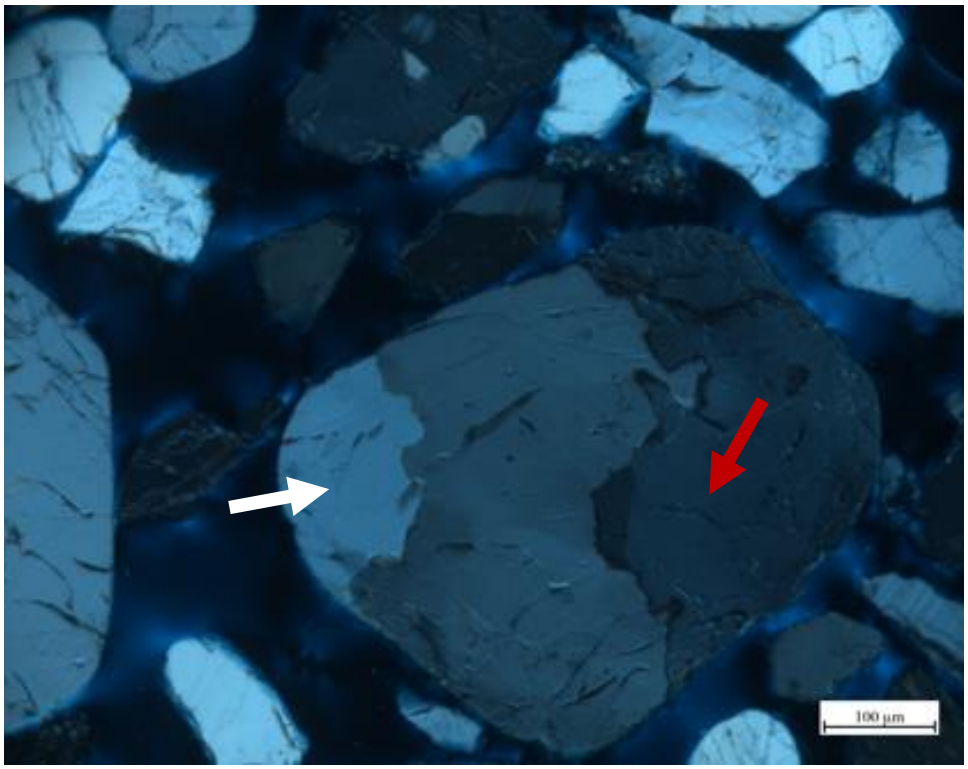

Figure 14. Strained Quartz (Lighter Portion – White Arrow And Darker Portion – Red Arrow within the Same Particle), XPL.

PCP1-CA

This coarse aggregate sample primarily made of pure limestone particles (Figure 15). However, a few limestone particles show the presence of siliceous impurity (Figure 16–Figure 18). The siliceous inclusions show the presence of both very fine cryptocrystalline quartz (ASR reactive, Figure 17) and medium grained quartz (almost non-reactive, Figure 17–Figure 18). These siliceous inclusions (especially the fine grained, Figure 17) inside the limestone particles can participate in ASR.

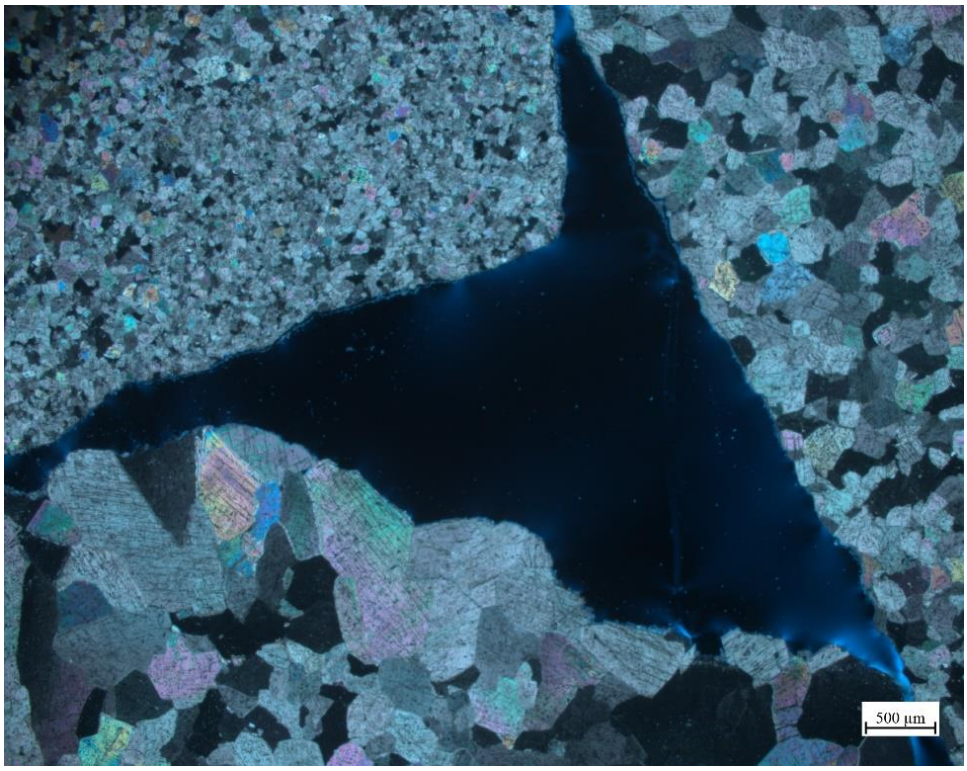

Figure 15. Limestone Particles, XPL.

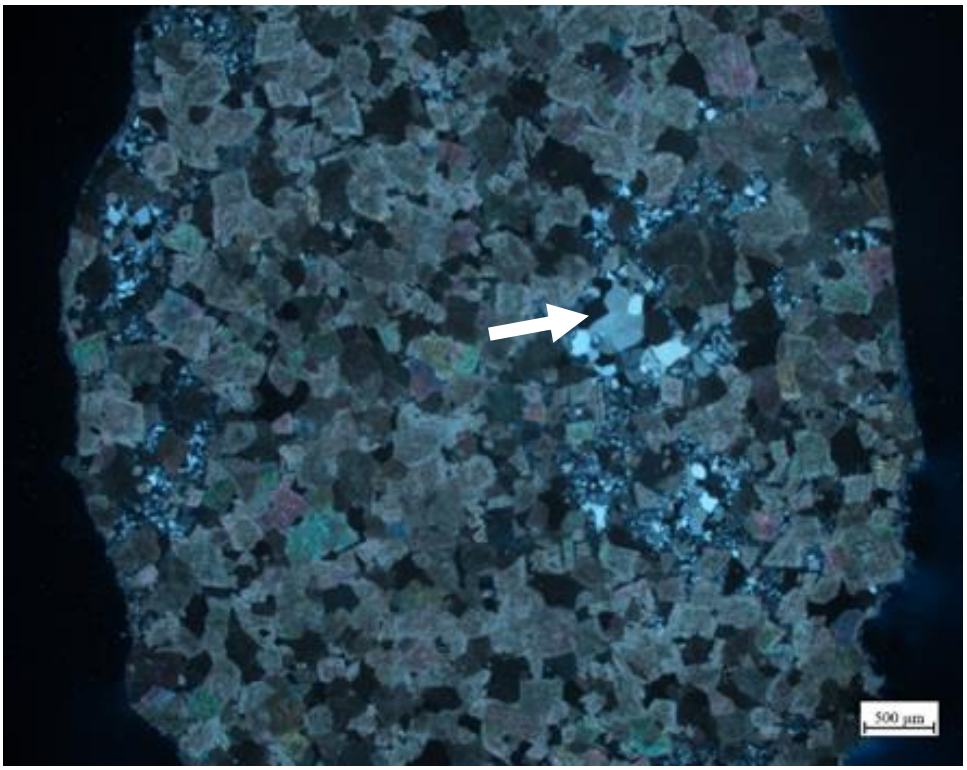

Figure 16. Siliceous Inclusions (White) within a Limestone Particle.

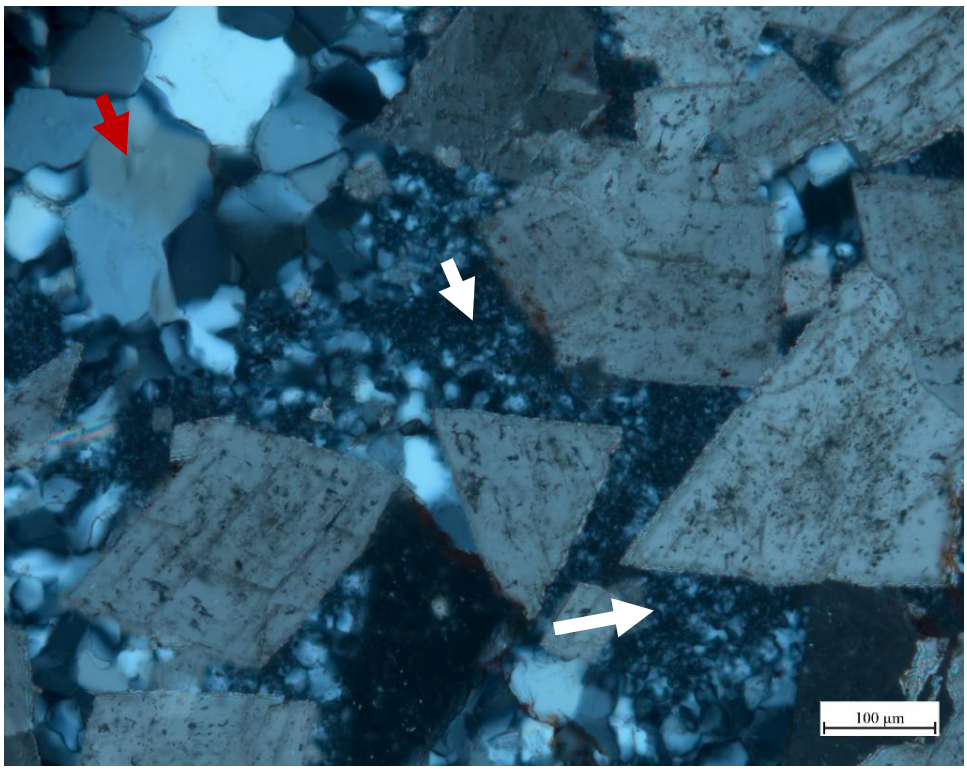

Figure 17. Fine Cryptocrystalline Quartz Inclusions (White Arrows) within the Limestone Particle in Figure 16. Note, the Presence of Medium Grained Quartz Parrticles (Red Arrow), XPL.

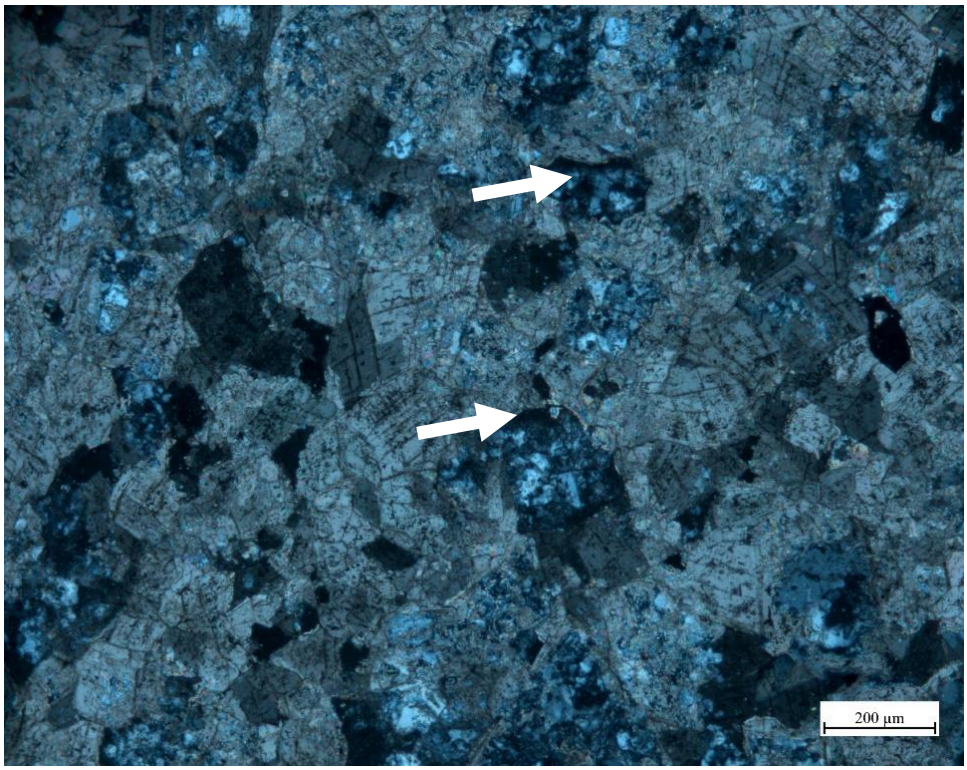

Figure 18. Relatively Coarser Siliceous Inclusions within a Limestone Particle.

PCP1-FA

This fine aggregate sample made of quartz, feldspar, chert, limestone, and some granitic particles (Figure 19):

- The presence of plenty of fine-grained chert particles (Figure 20) was observed and some of them can be ASR reactive.
- The presence of quartz with variable strain effects was manifested (Figure 21). The strained quartz can participate in ASR depending on degree of strain effects.
- Some sandstone particles show the presence of chert/chalcedony cementing materials in the interstitial space between grains (Figure 22). These fine cementing materials can be ASR reactive.

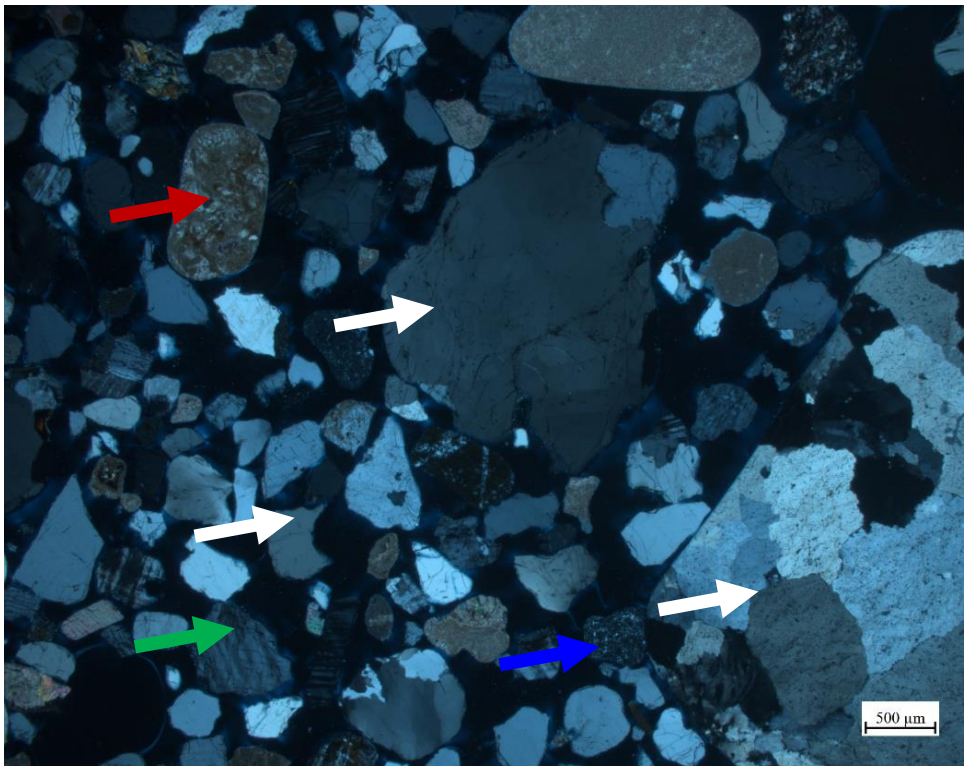

Figure 19. Quartz (White), Limestone (Red), Chert (Blue), and Feldspar (Green) Particles, XPL.

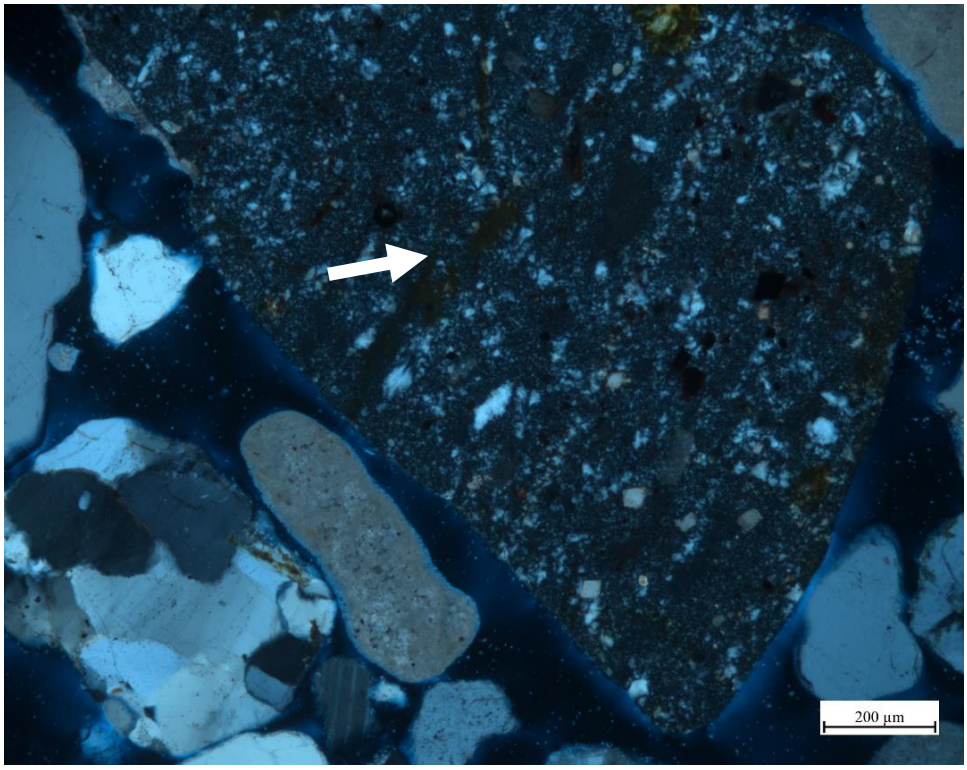

Figure 20. Fine Grained Chert Particle (White Arrow), XPL.

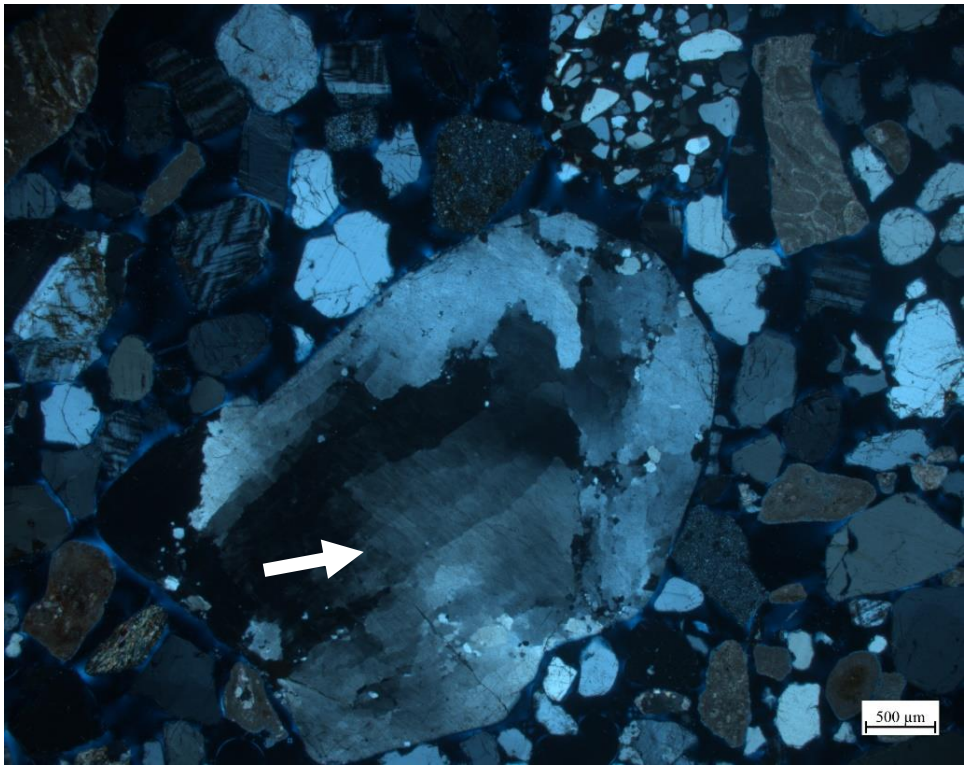

Figure 21. Strained Quartz (White Arrow), XPL.

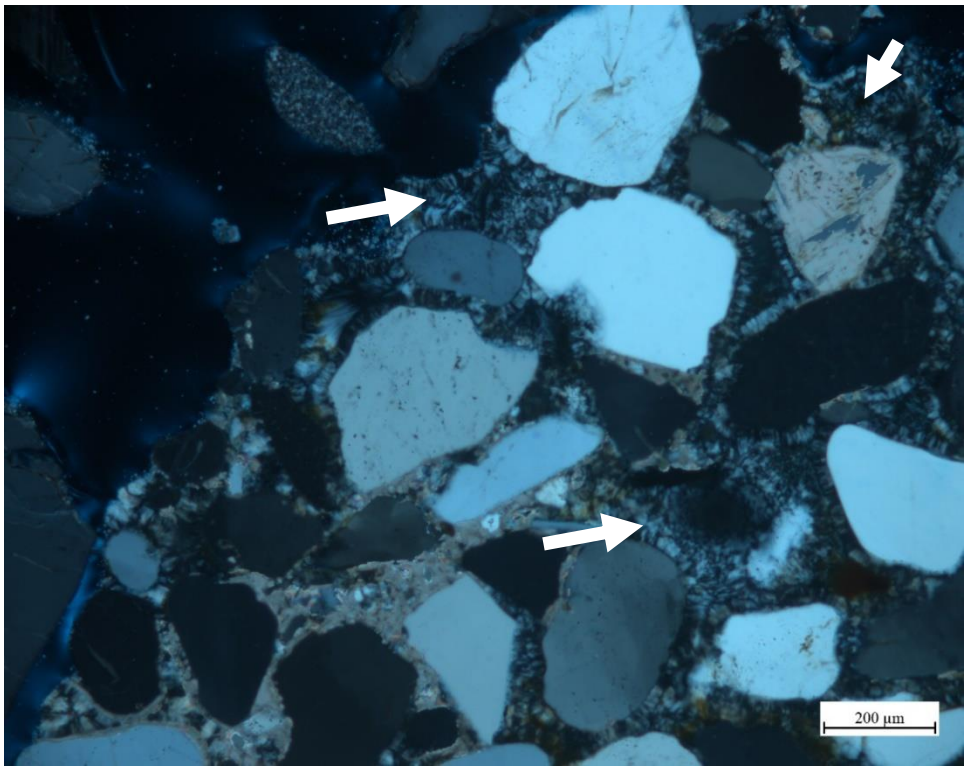

Figure 22. Presence of Chalcedony Type Cementing Materials (White Arrows) inside a Sandstone Particle, XPL.

PCP3-FA

This fine aggregate sample is made of chert, chalcedony, quartz, and limestone (very few) particles (Figure 23). The type of reactive siliceous constituents is described below:

- Chert, chalcedony, and strained quartz are ASR reactive.
- The presence of chert particles with varying particle sizes (i.e., coarse to fine) was observed (Figure 24). Grain size variation (coarse to fine) within a single chert particle was also observed at places (Figure 25).
- Strained quartz particles (Figure 23) also show variation in particle size as well as variation in strain effects.
- Not all chert and strained quartz particles can show ASR equally. The reactivity varies with the grain size in chert particles (the lower the grain size, the higher the reactivity) and strain effects (the higher the strain effects, the higher the reactivity) in quartz grains. In general, chert and strain quartz show slow – moderate reactivity. Fine-grained chert/chalcedony particle (greater in number in this sample) can initiate ASR at the beginning followed by contribution from stained quartz and sustain ASR in the long run. This kind of aggregate may not show significant ASR at the early stage but may show it at later ages.

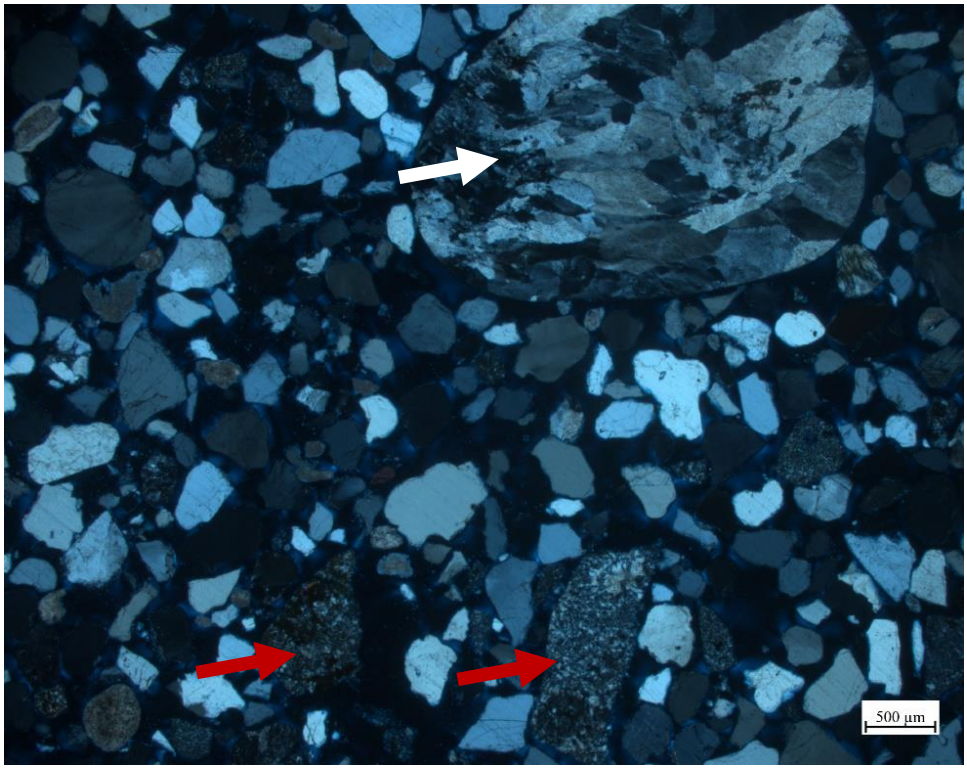

Figure 23. Strained Quartz (White) and Chert (Red Arrows) Particles, XPL.

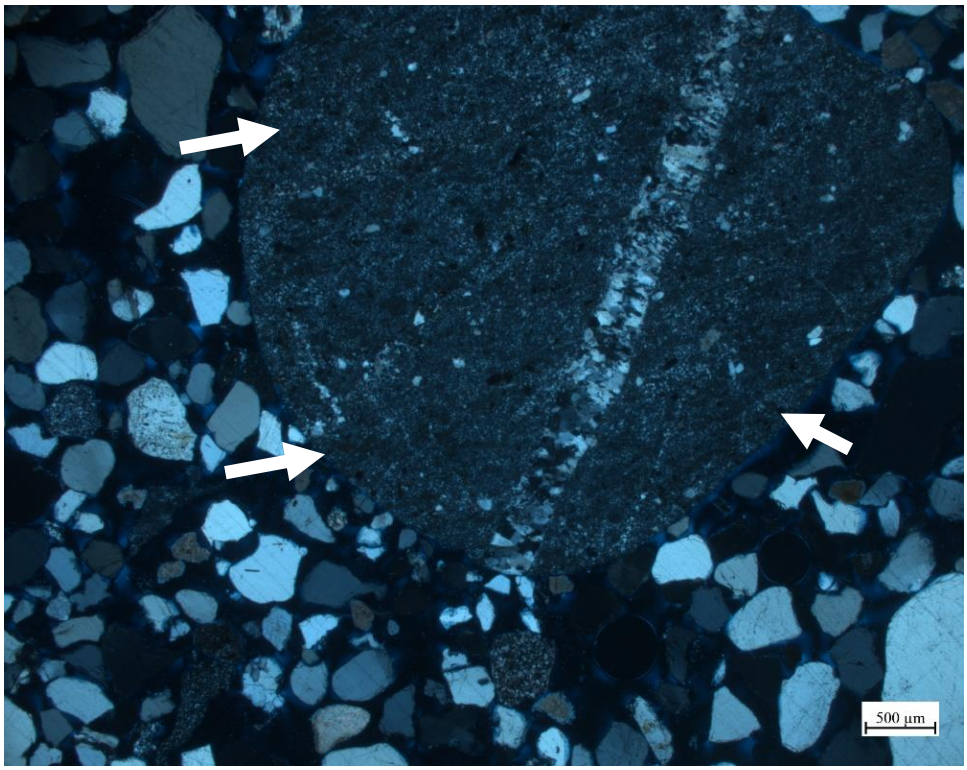

Figure 24. The Presence of a Very Coarse Chert Particle shown by White Arrows, XPL.

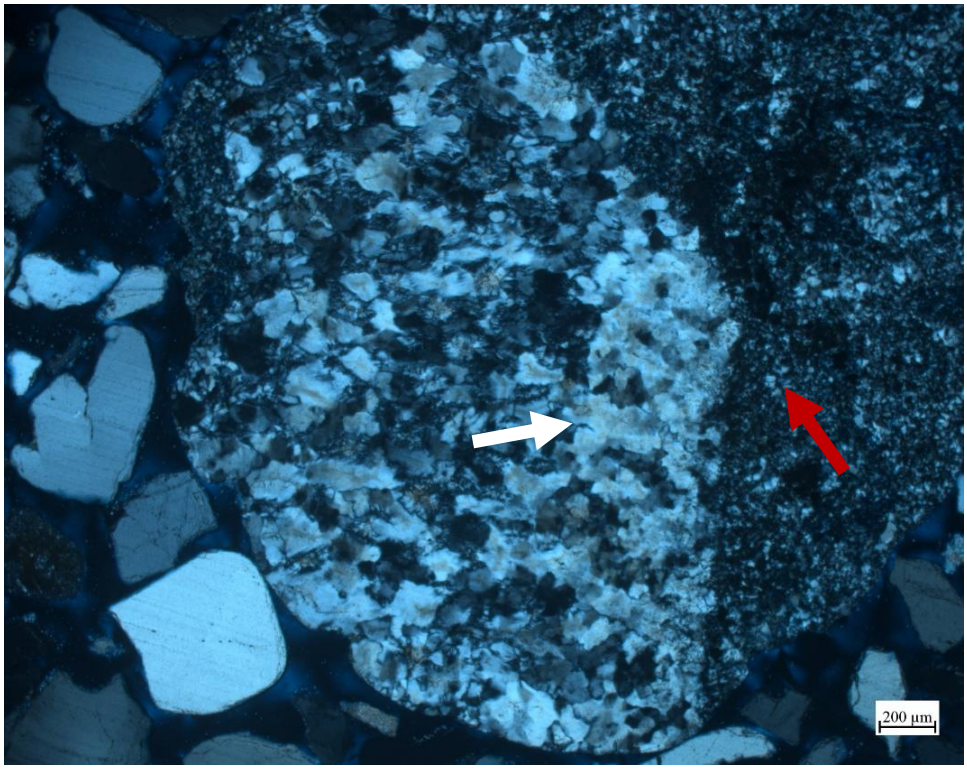

Figure 25. Grain Size Variation (Coarse: White; Fine: Red) within a Chert Particle.

PCP2-CA

This coarse aggregate is made of chert, metaquartzite containing strained quartz, and a few granitic particles (Figure 26 and Figure 27).

- Chert particles show size variability (very coarse to very fine). Individual particles show some inhomogeneity with respect to grain size (Figure 28–Figure 30). Finer-grained chert particles could show ASR relatively earlier, while coarse-grained chert particles take time to show ASR.
- The presence of strained quartz particles (Figure 31) with size variability (very coarse to fine) and variable strain effects was observed. ASR reactivity of strained quartz varies with strain effects.
- Fine-grained chert/chalcedony particles are greater in number.

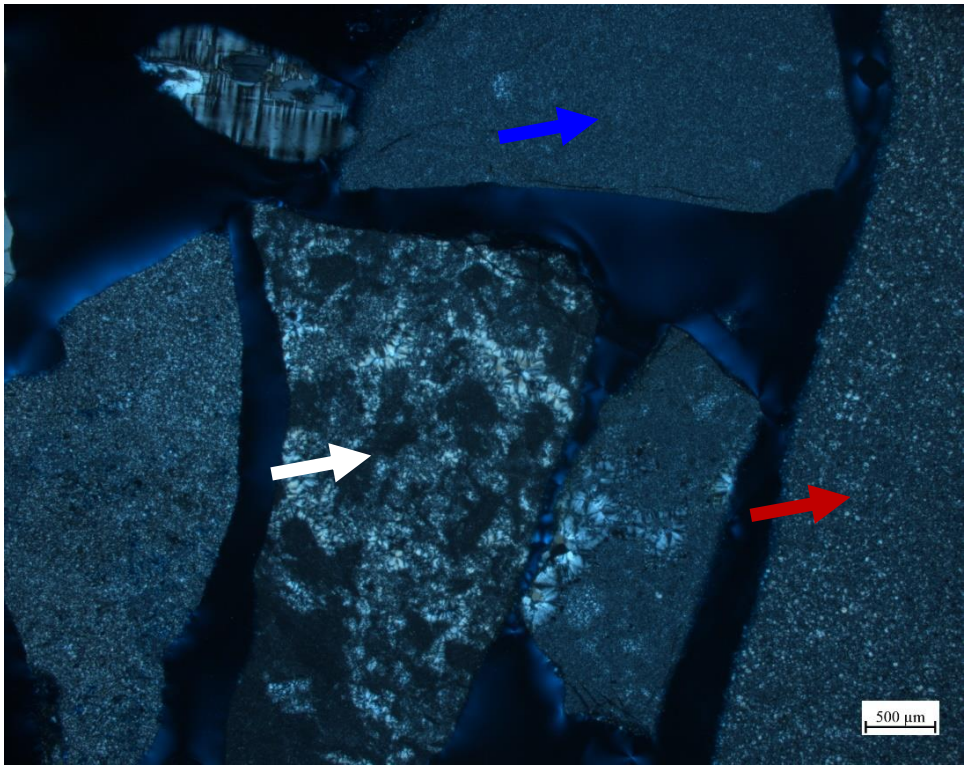

Figure 26. Chert Particles with Varying Grain Size (White: Coarse; Red: Medium; and Blue: Fine), XPL.

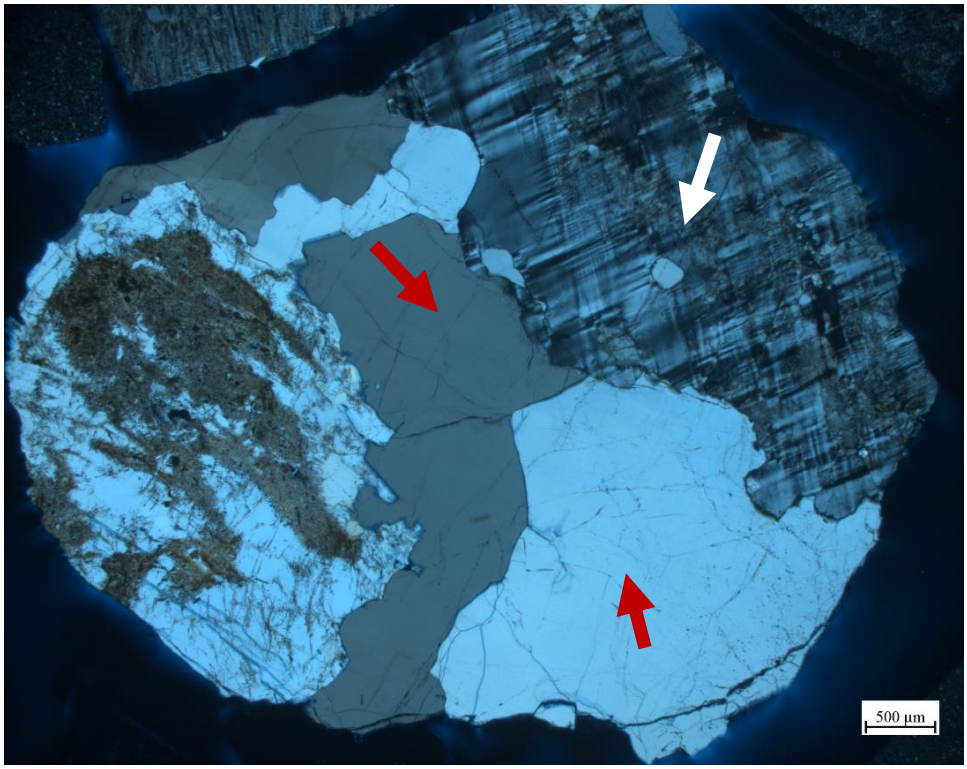

Figure 27. Granitic Particle (White Arrow – Feldspar, Red Arrows – Quartz), XPL.

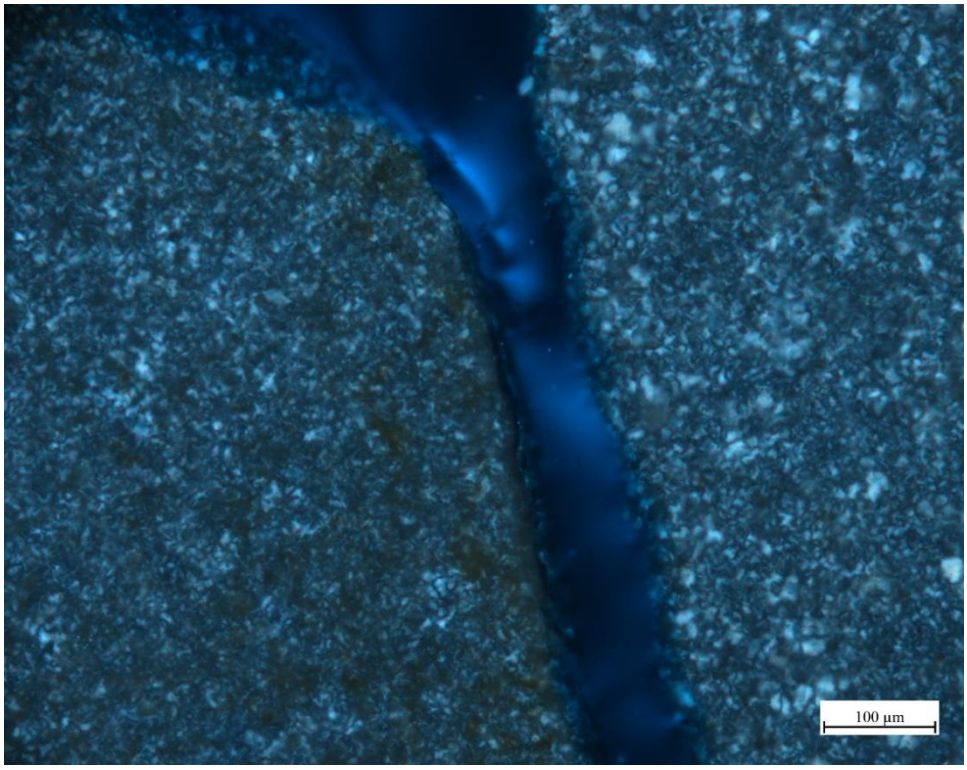

Figure 28. Appearance of Two Fine Chert Particles at Higher Magnification, XPL.

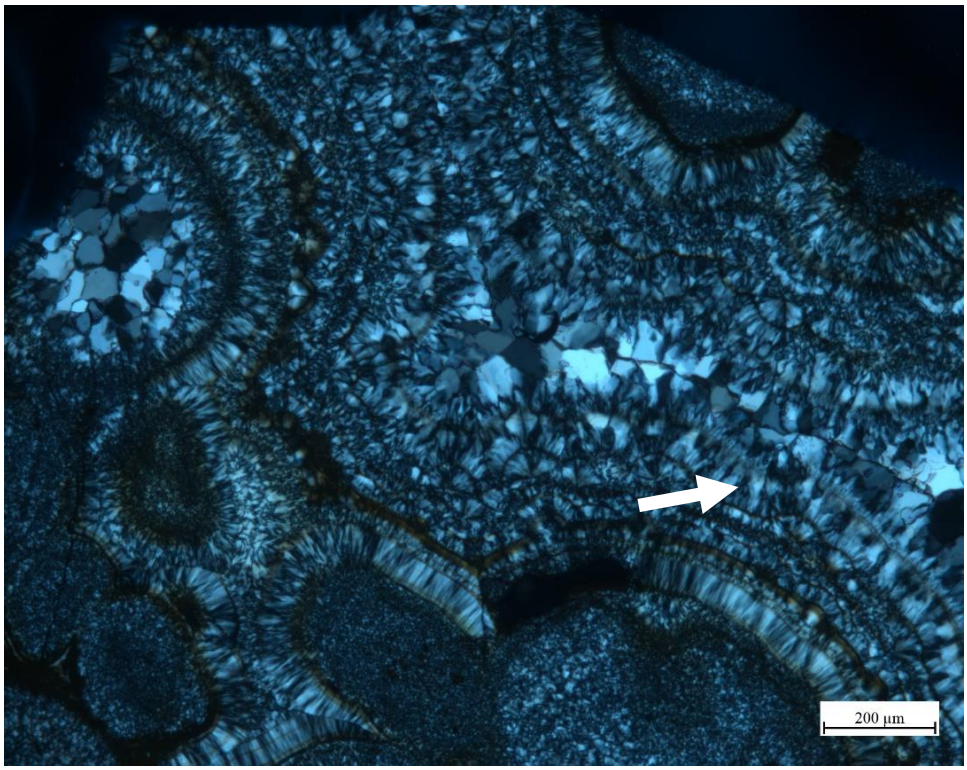

Figure 29. Appearance of a Coarse Chert Particle (Chalcedony Phases).

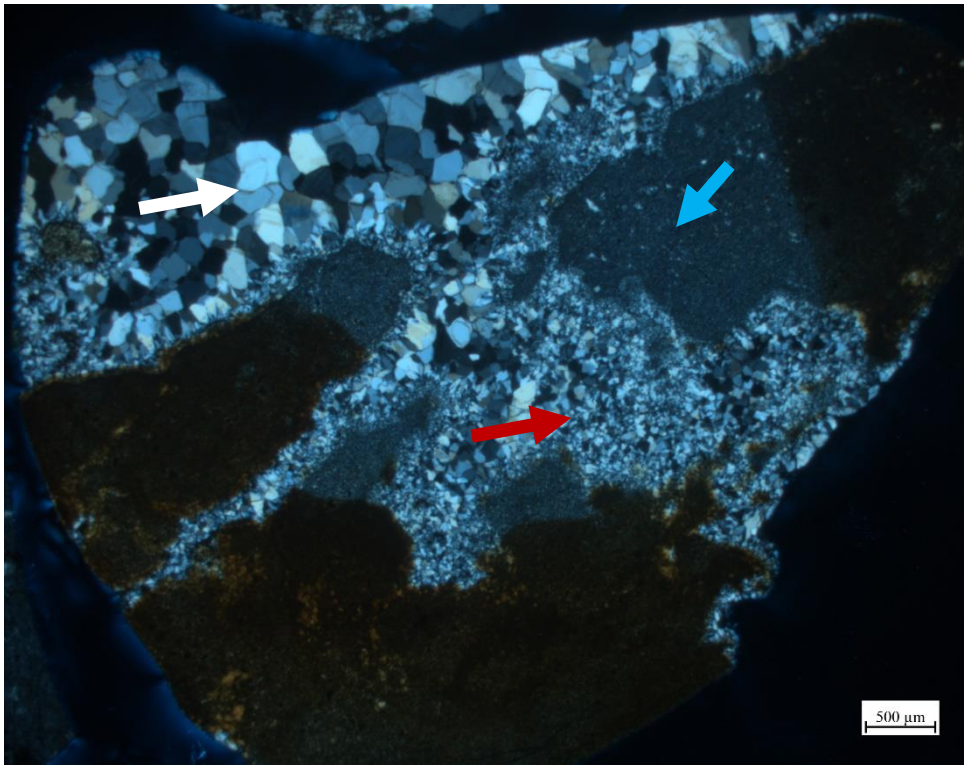

Figure 30. Grain Size Variation within a Chert Particle (Coarse Grained – White Arrow, Medium Grained – Red Arrow and Fine Grained – Blue Arrow), XPL.

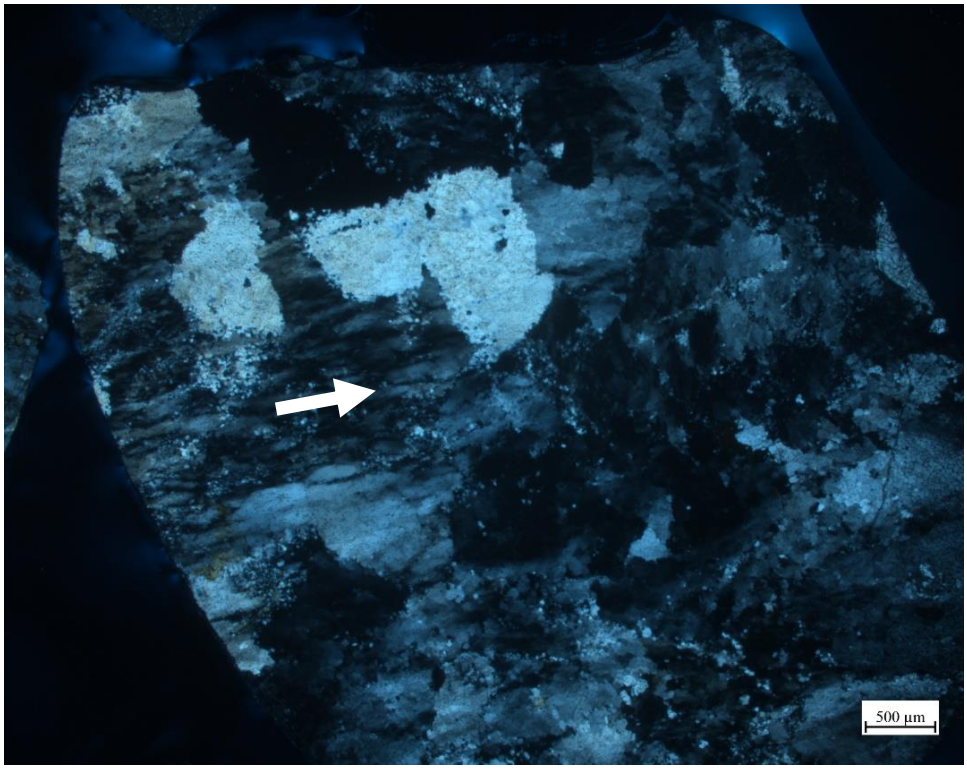

Figure 31. Strained Quartz (White Arrow), XPL.

APPENDIX B: VALUE OF IMPLEMENTATION

BENEFIT IDENTIFICATION

A Value of Implementation (VoI) analysis was completed at the end of this project to identify appropriate qualitative and economic benefits. Table 13 summarizes the benefit areas determined in this project, followed by a brief discussion for each selected benefit.

Table 13. Qualitative and Economic Benefits.

Selected	Functional Area	QUAL	ECON	Both	TxDOT	State	Both
	Level of Knowledge						
x	Management and Policy	x			x		
	Quality of Life						
	Customer Satisfaction						
	Environmental Sustainability						
x	Increased Service Life		x		x		
x	System Reliability and Sustainability		x		x		
	Improved Productivity and Work Efficiency						
	Expedited Project Delivery						
	Reduced Construction, Operation, and Maintenance Cost						
x	Locally Available Materials and Optimization			x			x
	Infrastructure Condition						
x	Engineering Design Improvement			x			x
	Safety						

Management and Policy

Policies for determining SCMs' (e.g., fly ash) replacement percentage to prevent ASR in different applications could change based on the aggregate reactivity, aggregate THA, and characteristics of the SCMs. This project provides technologies for developing a good ASR-resistant mix design and promoting overall good service life of precast concrete.

Increased Service Life

This project provides an effective way of tailoring ASR mix design depending on the level of protection needed. This process will ensure valuable resource conservation and help avoid paying for premium ASR protection when only minor protection is needed. The applied approach facilitates formulating ASR-resistant mixes, which ensures long-lasting durable concrete.

System Reliability and Sustainability

In 2013, around 92 percent of new bridges in Texas were built with precast concrete superstructures. Recently, TxDOT began adopting and implementing precast girder sections for extended span lengths of bridges as well. In order to prevent ASR distresses and maintain bridges in good condition, TxDOT needs to validate the mix design by incorporating design Options 1 through 5. In reality, replacement of 20 percent of the cement with Class F fly ash (Option 1) applies to all precast concrete. However, changes in coal composition along with application of control measures by thermal power plants to reduce environmental pollution is gradually leading to limited or no production of good-quality Class F ash in the future. This research can enable precast industries to prepare for when good-quality Class F ashes are no longer readily available and validate the use of different SCMs, thus helping TxDOT increase its system reliability by improving the service life as well as sustainability of precast concrete projects.

Locally Available Materials and Optimization

The use of blended coal (i.e., a blend of powder river basin and lignite coal) along with changes in power plant operations is a common practice by the coal-fired power plants to meet emission requirements. This practice has resulted in changes in fly ash composition and dwindling of conventional Class F ash in the market. This combined approach can be effective to do optimization of different types of SCMs to prevent ASR in a rapid and reliable manner and formulate case-specific, performance-based ASR-resistant concrete mixtures using locally available materials (e.g., fly ashes, aggregates).

Engineering Design Improvement

This applied approach can formulate performance-based ASR-resistant mixes and ensure long-lasting precast concrete. Since the locally available aggregate and SCM materials can be judiciously used and optimized with the applied approach, ASR distress can be minimized to a safer level. Therefore, engineering design on ASR preventive measures can be improved effectively.

VOI ESTIMATION

For VoI (Value of Implementation) submission, the expected value of savings per year has been generated according to the ASR repairing cost reported by TxDOT. Since the 2014 specification (item 789) was created, TxDOT spent a total of $200,000 on repairing damage related to ASR from 2017 to 2019. Therefore, it can be expected that around $100,000 per year can be saved through this implementation project.